DETECTION OF GLAUCOMA USING RETINAL FUNDUS IMAGES

A Dissertation submitted in fulfillment of the requirements for the Degree

Of

MASTER OF ENGINEERING

In

Electronic Instrumentation & Control Engineering

Submitted by

Disha Garg

801451006

Under the Guidance of

Sunil Kumar Singla

Associate Professor, EIED

2016

Electrical and Instrumentation Engineering Department

Thapar University, Patiala

(Declared as Deemed-to-be-University u/s 3 of the UGC Act., 1956)

Post Bag No. 32, Patiala – 147004

Punjab (India)

DECLARATION

I hereby certify that the work which is being presented in this thesis entitled, "**Detection of Glaucoma using Retinal Fundus Images**" in partial fulfillment of the award of degree of **Master of Engineering degree** in **Electronics Instrumentation and Control Engineering** submitted in ELECTRICAL & INSTRUMENTATION Engineering Department of **Thapar University, Patiala**, is an authentic record of work carried out by me under the supervision and guidance of **Dr. Sunil Kumar Singla, Associate Professor** of **Electrical and Instrumentation Engineering Department, Thapar University, Patiala**.

DATE: 15. July. 2016

Disha Garg

(Disha Garg)
801451006

I certify that the above statement made by the student is correct to the best of my knowledge and belief.

(Dr. Sunil Kumar Singla)
Associate Professor
Electrical & Instrumentation Engineering Department
Thapar University, Patiala

Countersigned By

(Dr. Ravinder Aggarwal)
Head
Department of the Electrical and
Instrumentation Engineering,
Thapar University, Patiala, Punjab.

(Dr. S.S. Bhatia)
Dean of Academic Affairs
Thapar University, Patiala,
Punjab.

ACKNOWLEDGMENT

In pursuit of this academic endeavor, I feel that I have been singularly fortunate because inspiration, guidance, direction, cooperation, love & care- all came in my way in abundance and it seems almost an impossible task for me to acknowledge the same in adequate term.

I am very thankful to the Director of Thapar University, Dr. Prakash Gopalan, and our Head of Department, Dr. Ravinder Agarwal, Department of Electrical and Instrumentation Engineering for their support during the research work.

Also, I shall be failing in my duty if I do not record my profound sense of indebtedness and heartfelt gratitude to my supervisor, Dr. Sunil Kumar Singla, Associate Professor, Department of Electrical and Instrumentation Engineering, Thapar University, Patiala, who guided and inspired me in pursuance of this work. It was his able supervision, advice and guidance from the very early stage of this research as well as giving me extraordinary experiences throughout the work which has resulted in fruitful outcome. I feel bereft of words to acknowledge his contribution to shape my academic perceptivity.

I am very thankful to Dr. Randhawa, Eye specialist, G.S Randhawa Eye Hospital, Patiala for his guidance and time he devoted on me to understand medical concepts.

I feel thankful to the entire faculty and staff of the Department of Electrical and Instrumentation Engineering. I would also like to thank my friends who devoted their valuable time and helped me in all possible ways towards successful completion of this work. I thank all those who have contributed directly or indirectly to this work.

Lastly, I would like to thank my parents for their unconditional support and encouragement.

(DISHA GARG)

ABSTRACT

Now a days Computer aided systems along with image processing techniques are used for the diagnosis and screening of various abnormalities in human body. Fundus image processing or Fundus Photography is one such technique which is used to examine the fundus of the Eye and detect its diseased conditions. Several eye disorders, like Glaucoma, are asymptomatic at the early stages. If not treated at appropriate time, it may lead to loss of vision. In order to prevent any such damage, it needs to be detected as early as possible.

The purpose of this research is the early detection of glaucomatous eye using the image processing techniques which are used to study size, shape and orientation of the fundus. The morphology of the fundus undergoes various changes in pathological conditions that can be examined with the help of Fundus Image processing. Fundus image consists of various features like Optic Disc, Optic Cup, Neuro-Retinal Rim tissue etc. The proposed methodology deals with extraction of Optic Disc (OD) and Optic Cup (OC) followed by calculation of the Cup-to-Disc Ratio. The image database used for this purpose has been collected from a local physician. By estimating areas of Optic cup and Optic disc, CDR ratio has been estimated. This ratio helps in isolating glaucomatous images from normal. After CDR calculation, Support Vector Machines (SVM) classifier using radial basis Gaussian function has been used in this methodology to classify the normal and glaucomatous eye. The accuracy of the algorithm has been found to be 98.33% and sensitivity is 100%.

LIST OF FIGURES

LIST OF ABBREVIATIONS

CDR- Cup-To-Disc Ratio

Fig- Figure

FN- False Negative

FNR - False Negative Rate

FP- False Positive

FPR - False Positive rate

IOP- Intra-Ocular Pressure

ISNT- Inferior Superior Nasal Temporal

NPV - Negative Predictive Value

NRRA - Neuro-Retinal Rim Area

OC- Optic Cup

OD- Optic Disc

OHN- Optic Head Normalization

ONH- Optic Nerve Head

POAG – Primary open angle glaucoma

PPV - Positive Predictive Value

RGB- Red Green Blue

RNF- Retinal Nerve Fiber

SE- Structuring Element

STARE- Structured Analysis of Retina

TN- True Negative

TP- True Positive

LIST OF TABLES

TABLE OF CONTENTS

CHAPTER 1

INTRODUCTION

Glaucoma is an immedicable neurodegenerative eye disease which leads to progressive damage of astrocytes and optic nerve fibers [1, 2]. It is the second most prevalent cause of vision loss. About 60 million people are suffering from this disease [3]. This is because of late detection and diagnosis as patients are asymptomatic till the late stage. Optic nerve fibers which is damaged is irreversible so it is important to diagnose at early stage and give the subsequent early treatment to prevent the consequences.

Clinically, there are various methods to diagnose glaucoma like analysis of patients' medical history, by measuring IOP, by assessing ONH manually [3] etc. For an early detection of Glaucoma there is need for an economic and efficacious screening system.

Medical image processing advancements have permitted the development that is based on Computer-aided diagnosis systems [4]. Main focus here is to estimate vertical optic cup-to-disc ratio (vCDR). Other than CDR, many other pathologies are also used for detection of glaucoma. Neuro retinal rim (NRR) is one such feature which is looked for the `ISNT Rule'; it's dwindling in different quadrants (Inferior, Superior, Nasal and Temporal); Retinal Nerve Fiber Layer (RNFL) defects and Parapapillary Atrophy (PPA) [5] etc.

1.1 GLAUCOMA

Glaucoma is a group of eye diseases that is associated with an increased fluid pressure, the Intra-Ocular Pressure (IOP). This results in optic nerve damage. The IOP is measured by a tonometer [1, 2] and ranges from 10-21 mm Hg normally. An increased eye pressure is used for screening of glaucoma, being its major risk factor. Elevated eye pressure damages the delicate blood vessels and nerve fibers including the optic nerve as shown in Figure 1.1.

The part of eye in front of lens is divided into anterior and posterior chambers. A transparent fluid, called the aqueous humor, flows through them and provides nourishment to the surrounding trabecular meshwork. It is first discharged in the posterior chamber by the ciliary bodies. Then it flows into the anterior chamber between the iris and the cornea through the pupil and enters into episcleral vein as shown in Figure 1.2. From here it drains through trabecular which is located at base of iris.

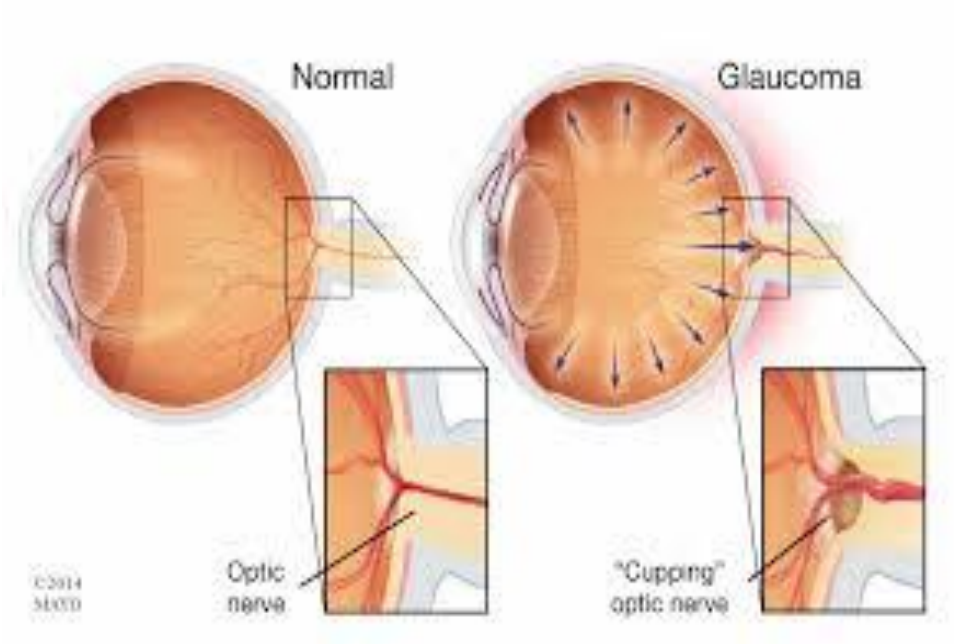

Fig 1.1 Damage of Optic nerve due to higher eye pressure [6]

The rate of secretion is equal to the rate of drainage in a normal eye. This drainage channel is blocked in a glaucomatous eye. Due to this blockage the fluid does not drain out and gets accumulated in the chambers. Due to this, the IOP in the chamber increases which pushes the lens back on the vitreous humor which leads to compression of the blood vessels and the nerve fibers including the optic nerve. As a result, there is partial loss of vision and if it is not treated which may cause total blindness.

1.2 TYPES OF GLAUCOMA

The various types of Glaucoma are given below:

1.2.1. PRIMARY OPEN ANGLE GLAUCOMA

There are no indications related to Primary Open Angle Glaucoma. Intraocular pressure (IOP) increases slowly and there is no swelling when cornea is transformed [7]. While if the cornea tumefies, then signs and symptoms of this disease can be seen. But this disease often goes unnoticed. POAG has a feature that it is free of pain because of which it gets unidentified until it is too late. There is irreversible damage of vision by then.

The trabecular meshwork appears to be normal clinically. But because of ageing, cell number and their ability to perform their normal function decreases. One school of thought believes it is because of structural defect in the drainage system of the eye. Other believes it to be

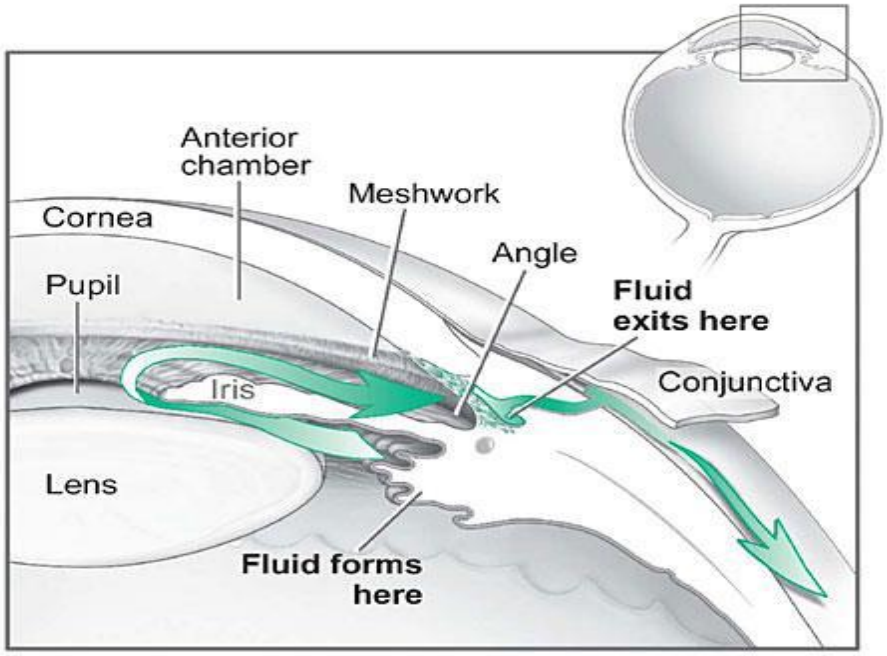

Fig 1.2 Aqueous fluid pathway [8]

an enzymatic problem. Various research centers are evaluating these theories.

In Glaucoma, there is an increase in IOP leading to various problems. In a normal individual, the IOP up to 21 mm Hg is considered normal. If the pressure raises to 22 then it is suspicious. However, patients with increased IOP do not develop glaucoma. This variation from individual to individual is still under research.

As discussed earlier, increased IOP damages the optic nerve cells which results in formation of blind spots in visual field [7]. These first develop in the peripheral field of vision. Later, the central vision is affected. This may cause an irreversible loss of vision because the nerve cells once dead cannot be restored. So, it is necessary to detect glaucoma at early stage. As we proceed, we will talk about various ways to diagnose glaucoma. In Figure 1.3 Primary Open Angle Glaucoma has been shown.

POAG is a chronic genetic disorder. It cannot be cured permanently but can be restricted or slowed by proper treatment. Chemotherapy is crucial in preventing damage leading to vision

loss. But the problem associated with the disease is lack of symptoms and thus lack of awareness among patients to continue the expensive treatment lifelong. Also, there are many bothersome side effects of chemotherapy which should be discussed with a physician.

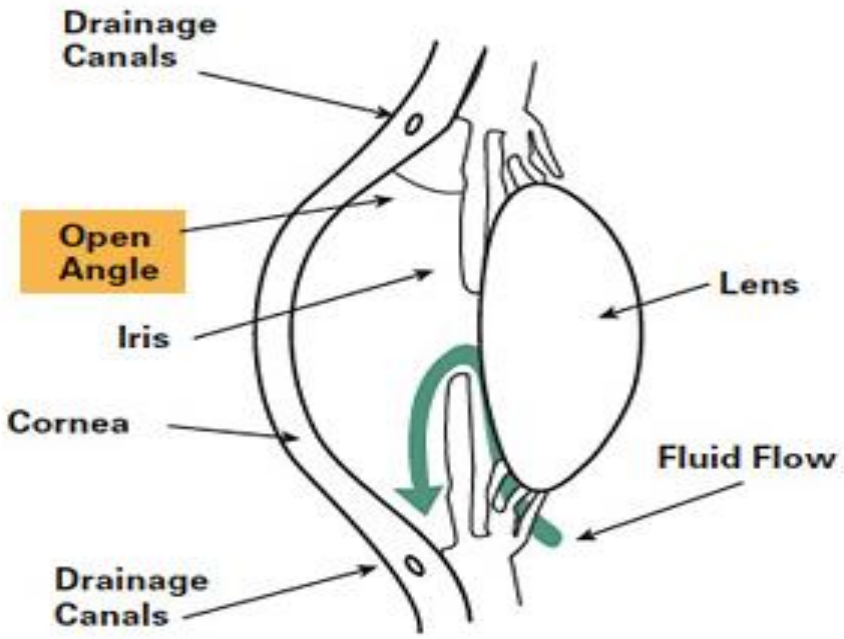

Fig 1.3 Primary open angle glaucoma [9]

1.2.2. NORMAL TENSION GLAUCOMA

Normal tension or low-tension glaucoma is characterized by gradual optic nerve damage and loss of visual field. The Intraocular pressure (IOP) remains normal [10].

It occurs due to decreased blood flow to the optic nerve. This results in apoptosis of cells (cell death) which are responsible for impulse transmission from retina to brain. Also, such eyes become susceptible to damage even when pressure is in high normal range.

Since the proper treatment for this condition is largely unknown, study is being conducted in this context called the International Collaborative Low Tension Glaucoma Protocol. Research on the blood flow to the optic nerve and its importance in glaucoma is helping to develop new methods for treating this disease.

1.2.3. ANGLE-CLOSURE GLAUCOMA

In this type of glaucoma, the anterior chamber of the affected person is smaller than normal. The angle is 45 degree mostly. There is a direct relation between the angle and the distance between the iris and trabecular meshwork. As the angle gets narrower, so the distance becomes closer. Angle closure glaucoma has been shown in Figure 1.4.

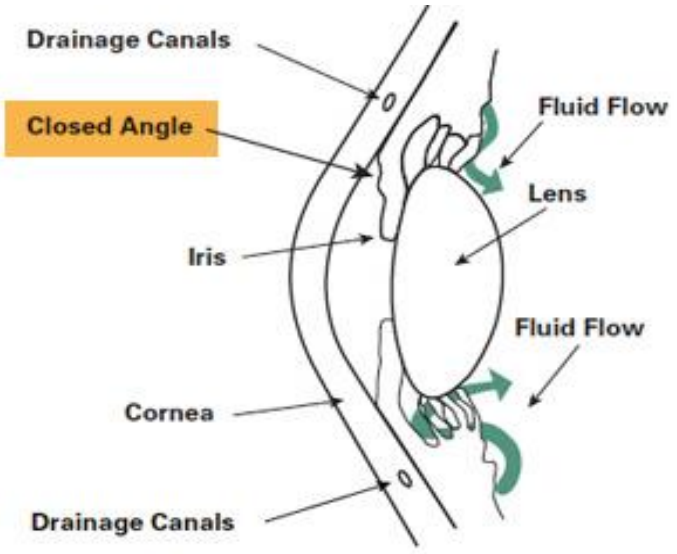

Fig 1.4 Angle closure glaucoma [11]

Lens grows with age gradually. There is decrease in the flow of aqueous humor between the iris and lens, increasing the fluid pressure behind the iris. This further narrows the angle.

1.2.4. ACUTE GLAUCOMA

In acute angle-closure, IOP increases suddenly unlike POAG, where it increases slowly. This sudden increase in pressure can takes place in few hours and is very painful [12]. Sometimes, patient starts feeling nauseated when pain is very severe.

The symptoms include redness of eyes, swelling and clouding of cornea and blurred vision. An attack of Acute Glaucoma is an emergency condition where permanent loss of vision can occur, if the treatment is delayed. Cataract is another associated condition. Dark environments such as movie theaters are commonly associated with such attacks. Darkness causes dilation of the pupil i.e. it increases in size narrowing the angle and initiating an attack. Many acute attacks occur due to stress as the pupil also dilates during anxiety or excitement. Also, various drugs can

dilate the pupil leading to a sudden attack of glaucoma such as anti-depressants, antihistamines, medicines for cold and for nausea.

These attacks may not always be major and can occur as a series of minor attacks in some cases. These are associated with slight blurring of vision along with haloes i.e. rainbow-colored rings around lights are seen but are usually painless and without redness. They are stopped when the patient enters an enlightened room or sleeps as in both the situations the pupil constricts naturally, thus leading to the pulling away of iris from the drain.

Gonioscopy is a technique that can help in predicting susceptibility of a subject to acute attacks. In this, a special lens containing a mirror is used to examine the width of the angle by placing it in front of the eye. Patients having narrow angles are susceptible to acute attacks and need to get treatment at early stage.

This condition can be treated with eye-drops which help in constricting of the pupil and chemotherapy that reduces the fluid production in the eye. Once the IOP is controlled to a safe level, a laser iridotomy can be performed. In this procedure, a small opening is created in the iris using a laser beam allowing free flow of the fluid. This is a painless process as the eye is anaesthetized with drops. This whole procedure takes thirty minutes or less. In most of the cases, both eyes have narrowed angles, so the normal eye is also operated upon as a prophylaxis.

But every angle-closure glaucoma patient not necessarily suffers from an acute attack. Sometimes there can be development of chronic angle-closure glaucoma [11]. Here, no obvious symptoms are present as there is gradual closure of iris over the drain. Scars develop slowly between iris and drain and a sufficient amount of scar tissue is required to cover it. Drugs like pilocarpine prevent an acute attack but they do not stop growth of chronic form of the disease [12].

1.2.5. PIGMENTARY GLAUCOMA

Pigmentary glaucoma is an open-angle glaucoma which is hereditary in nature [13]. It is more common in males than in females. It mainly begins in the early middle age, causing threat to normal vision. The anatomy of the eyes is said to be the reason behind the development of this glaucoma. Nearsighted patients are more susceptible. Nearsighted eyes, clinically called myopic eyes, have a concave-shaped iris resulting in a wide angle. The pigment plugs the openings of meshwork resulting in clogging resulting in increased IOP.

The treatment for this condition is Miotic Therapy, but these drugs can cause visual blurring in young patients if used in drops form. Thus a slow-release form is preferred.

1.2.6. OCULAR HYPERTENSION

In this condition, increased IOP is present but there is no optic nerve damage or loss of vision.

1.2.7. SECONDARY GLAUCOMA

As the name indicates, it originates from previous eye disease. Patients with tumor or on prolonged steroid therapy are prone to this glaucoma.

1.2.8. CONGENITAL GLAUCOMA

It is mainly found in infants and young children. Inheritance may be a common factor. It is not so frequent in nature. Chemotherapy is not indicated due to side effects and so conventional surgery is the treatment of choice [14].

1.2.9. EXFOLIATION SYNDROME

It is abundantly found all over the world, but European people are the most affected ones. It is common in people of age over 50 years [15]. Here, the movements of the iris rub off white material along with pigment from the lens. Both clog the trabecular meshwork elevating IOP.

This syndrome may result in both angle-closure glaucoma and open-angle glaucoma in the same subject. But exfoliation syndrome patients are six times more susceptible than the normal individuals. One eye is often affected long before the other, reasons being unknown. Detection of this syndrome before the development of glaucoma helps in minimizing the chances of vision loss.

1.2.10. TRAUMA-RELATED GLAUCOMA

Trauma is one of the many reasons that cause glaucoma like a blow to the eye, penetrating injury or chemical burn. This occurs due to physical wear in the drainage network of the eye [14]. It is, thus, important for a person suffering an eye trauma to get routine examinations done at regular intervals.

1.3 RISK FACTORS OF GLAUCOMA

Various factors are responsible for causing Glaucoma. Old age is one of the most important cause as people above 60 are more susceptible. Previous eye disorders like tumors, eye injuries, myopia etc. increase the risk of glaucoma. Prolonged use of corticosteroids make the patients more prone to glaucoma [16]. Chronic ailments like diabetes, peripheral vasospasm and migraine may also result in glaucomatous condition.

1.4 DIAGONOSIS

It includes the patient's complete family and medical history, examination of thinner cornea, assessment of increased IOP and Optic Nerve head (ONH) [3]. Ophthalmoscope is used to examine optic images called Fundus images to evaluate the changes in ONH. Some overt features present in these images, as shown in Figure 1.5, are analyzed to specify it as normal or Glaucomatous eye.

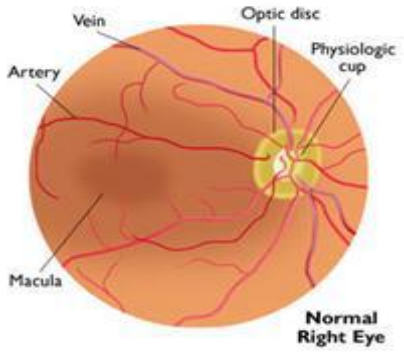

Fig 1.5 Healthy Fundus [17]

Optic disc (OD) is one of the most important features to be noticed which is elliptical in shape and orange-pink with a pale center in a normal retinal fundus image. In pathological conditions, this orange pink color starts getting pale representing unhealthy neural tissue. The Optic disc (OD) or optic nerve head is the point of exit for ganglion cell axons leaving the eye. Optic Cup (OC) is the white center in optic disc. The CDR is the ratio of diameter of cup to that of the disc. This ratio is widely used to detect Glaucoma. The range for a healthy eye varies from 0.3 to 0.5. This value increases with the optic nerve damage and there is complete vision loss when it reaches 0.8 [3].

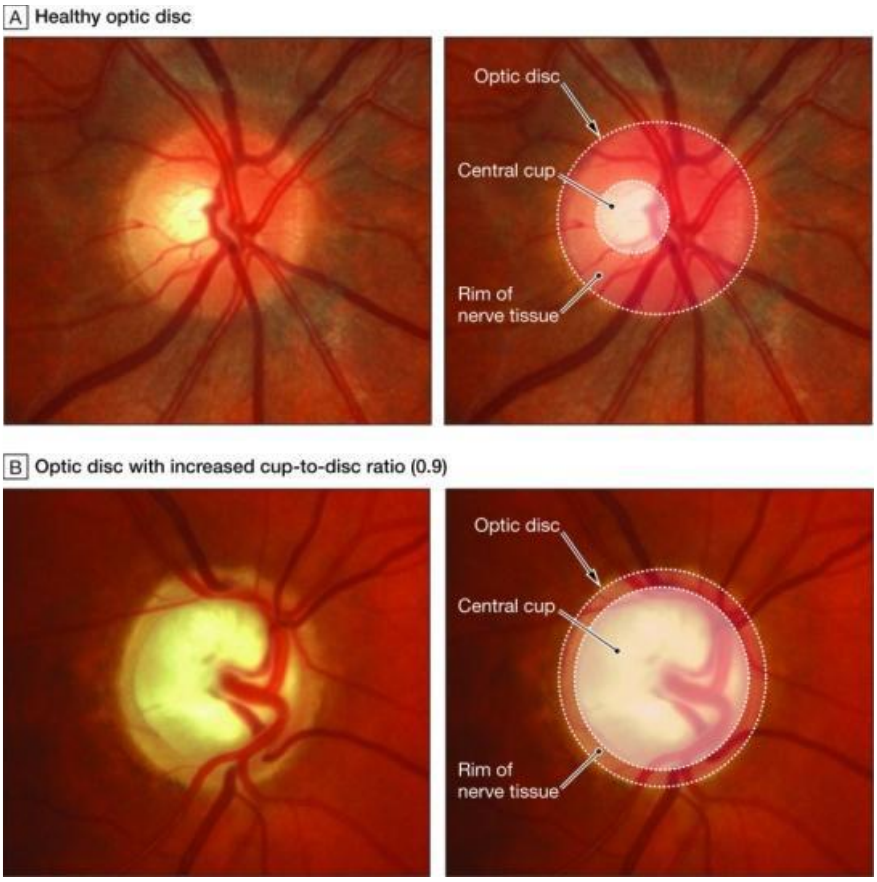

Fig 1.6 Optic disc (a) Healthy (b) Unhealthy [17]

Figure 1.6(a) and (b) shows a comparison between a healthy Optic disc and unhealthy Optic Disc. But CDR is mainly used for screening glaucomatous cases. CDR more than 0.5 is categorized as suspicious while less than 0.5 as normal. Subjects under suspicious category only are considered for further tests where Neuro-Retinal Rim (NRR) and ISNT Quadrants are studied for confirmation.

In Healthy fundus, the areas of various regions of Neuro retinal rim are such that area is maximum in inferior region compared to that in superior region which in turn is more than that of nasal region area and the temporal region has minimum area [18]. ISNT rule of a Healthy fundus has been depicted in Figure 1.7. However, In Glaucomatous fundus this rule is violated.

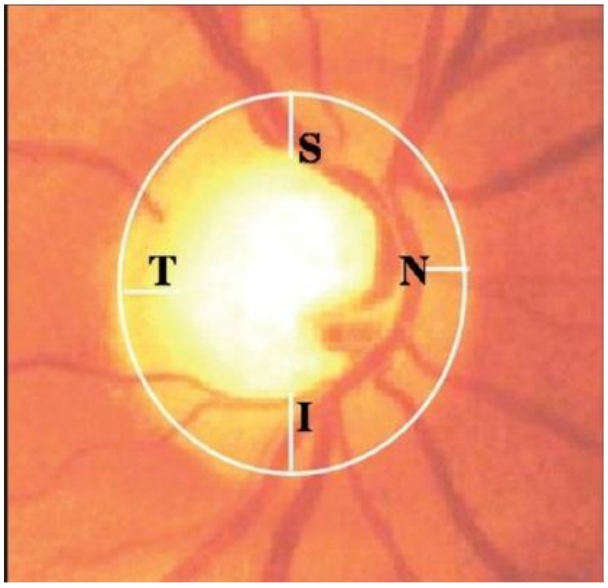

Fig 1.7. ISNT rule [18]

1.5 OBJECTIVES OF THE DISSERTATION

The objectives of the dissertation titled "Detection of Glaucoma using retinal fundus images" are:

- To study the various features of retinal fundus images.
- To differentiate between normal and glaucomatous fundus images.
- To analyze various fundus images in order to find out the Glaucomatous eyes.
- To classify the images into Normal and Glaucoma image using Gaussian radial basis kernel.

CHAPTER 2

LITERATURE REVIEW

From past few years, research has been carried out to develop various techniques for automated detection of eye disorders like Glaucoma at early stages. Failure to do so may result in complete vision loss. Hence, many researchers have studied and proposed various methods for the application of digital image processing. Some of them have been described in this section.

James Lowell et al. [19] proposed an algorithm for optic disc localization and segmentation of Optic Nerve Head (ONH). For this template matching and deformable contour model has been used. After segmentation, detection of diseased fundus has been done by the contrasting features of optic disc. This has been done in fundus images with low resolution.

Kevin Noronha et al. [20] proposed various methods to highlight the contrasting features of fundus like optic disc, exudates, fovea etc. The center of optic disc has been detected by using Hough transform and other features have been detected using different morphological operations. After applying morphological operations diseased fundus is detected by examining the features of optic disc.

Peng et al. [21] stated that edge enhancement of the fundus images can be done using transform based techniques in low-resolution images. This results in change of main features of the image for detection. This change in features have been used in order to detect the glaucomatous fundus.

S. Shekhar et al. [22] described a computer based image analysis technique to localize optic disc which involves two steps. Firstly, the morphological processing is used to extract the brightest region of image. In the second step, optic disc is detected using Hough transform to extract out the circular region of interest.

G.B. Kande et al. [23] used geometric active contour and maximum local variance in order to detect boundary of optic disc of the fundus and to locate a point respectively. He has used different methodologies for segmentation of optic disc. He followed a methodology where image is converted to Hue Saturation Intensity (HIS). In this median filter has been used to remove the level of noise.

Ahmed W. Reza et al. [24] proposed an algorithm in which certain operation are followed. Firstly, in order to blend the low intensities, averaging filter has been used after which contrast adjustment has also been applied to make it different from the background. In this algorithm morphological operation, minima imposition, maxima operator and watershed transformation has been used.

Jagadish Nayak et al. [25] proposed a method in which RED and GREEN parts of the fundus were extracted out which represent disc and cup respectively. For separation of cup and disc, threshold values and standard deviations have been used. Before separation, morphological operations were also performed on the image.

S. Ravishankar et al. [26] proposed an algorithm for detection of optic disc. In this study, localization of various features of fundus image has been done by using morphological operations. After the detection of disc, removal of blood vessels has been done to locate the optic disc.

Rudiger Bock et al. [27] examined pixel intensity values and many other parameters. Here the image is resized to 128 x 128 pixels. For this purpose appearance based dimension reduction technique has been used. Histograms were used to show the change in CDR values.

Arturo Aquino et al. [28] detected boundary of the disc using Circular Hough Transform. For the extraction purpose the disc pixel and its neighboring area is taken into account. From the fundus, the selected area is extracted and then out of this OD is taken out by location method by estimating the boundaries by Circular Hough Transform.

D.W.K. Wong et al. [29] proposed a scheme to extract OD out of retinal fundus by applying supervised learning. In the presented algorithm after segmentation, classification with the help of SVM has been done. Local neighborhood and local pixels are used for the segmentation purpose.

Ahmed E. Mahfouz et al. [30] presented his work to estimate the boundary of the disc by encoding the x and y coordinates. This segmentation method is faster than the regular localization techniques and takes less than a second for disc localization. The work was carried on STARE and DRIVE data bases available publically.

P.C. Siddalingaswamy et al. [31] proposed an algorithm to detect optic disc thereby detecting the diameter and center of disc. In this algorithm, various features of fundus images were detected which include blood vessels, OD, and fovea.

Madhusudan Mishra et al. [32] deduced the pathological procession of glaucomatous fundus by calculating CDR using active contour method. Here active contour and multi thresholding methods have been used in order to detect OC and OD. For the given methodology after the illumination correction, blood vessels are removed from the pre-processed image because they do not play any role in detection of glaucoma. Threshold values are assigned to both cup and disc. In addition, assignment is such that cup is given higher value for thresholding than that of disc. In the end, CDR is calculated by using mathematical functions from the cup and disc values.

A.W. Reza et al. [33] extracted the features using watershed segmentation. In this algorithm, OD exudates and cotton wool have been extracted using marker-controlled watershed segmentation. Apart from extraction, pre-processing of image, filtering and adjustment of the image taken has also been done.

Feng shou Yin et al. [34] proposed method for segmentation of OD from the fundus sample of retina using edge detection, Circular Hough transform and statistical deformable technique.

Jun Cheng et al. [35] used elimination method for segmentation, which in turn has been done using elliptical Hough Transform. Along with Hough Transform, edge filtering and peripapillary atrophy has also been done in this proposed methodology to segment the OD. With this, the structures not belonging to disc are eliminated for more accuracy.

A Dehgani et al. [36] presented a novel approach in which segmentation is done by detecting the boundary of optic disc. This method is easier for segmentation because in this firstly blood vessels are removed which are not of our concern followed by estimation of center of disc.

M. Esmaeili et al. [37] proposed an algorithm in which the extraction is done by using DCUT and curvelet transform. Optic disc is distinguished from other retinal fundus features by bright lesions. It is a three stage process.

S. Kavitha et al. [38] presented a technique to detect glaucoma by estimating NRR and Optic cup. This methodology has used K means clustering. The boundary of cup and disc can be differentiated using K means clustering. The features based on shape are used as input to ANFIS which is then used for the purpose of classification.

H. Yu et al. [39] presented a methodology in which Template matching has been used. This is used to locate optic disc by using different image resolution. Morphological operations are also

performed to highlight and remove the blood vessels from the retinal fundus. Further, they are used to fill the gaps.

M.R.S.P. Kumara et al. [40] proposed an algorithm which is based on active contours or snakes. In this methodology optic disc boundary is estimated using Circular Hough Transform and morphological operations. In the end, extraction in this proposed methodology is done by using active contour model.

Fauzia Khan et al. [41] presented an algorithm for early detection by extracting V plane from HSV image, which further helps to detect OD and OC. In this, the image is first converted to gray image whose mean value is calculated to set the threshold value. OC and OD have different threshold values because brightness changes from cup to disc.

Ana Salazar Gonzalez et al. [42] proposed a simple and novel method for segmentation. In this, blood vessels are removed by Markov Random field image restoration. After removing the vessels from the retinal fundus, compensation factor method is used for the extraction of disc.

CHAPTER 3

PROPOSED METHODOLOGY

In this study, 120 sample images have been collected from an ophthalmologist to screen a Fundus image. The Optic Disc and Optic Cup along with their areas have been extracted from these images. The algorithm developed in MATLAB R2015a has been used for this purpose.

The areas acquired from this are divided to get the Cup-to-Disc Ratio. Therefore,

Cup-to-Disc Ratio (CDR) = (Cup Area) / (Disk Area)

This ratio is used to sort the images into normal or glaucomatous. For normal subjects, the ratio is between 0.3 to 0.5 and if the ratio is more than 0.5 then they are said to be at risk. Classification of the images has been done using radial basis Gaussian support vector machine classifier.

Analysis of the algorithm proposed in this dissertation has been done by a Confusion matrix.

3.1 Basic Methodology

The Cup-to-disc Ratio (CDR) is a significant feature for detection of Glaucoma. It determines whether the subject is at risk or not. For this, the colored RGB images of suspicious samples have been changed into Gray scale images. Morphological operations are then carried on these images for examining OD and OC. Then the so obtained CDR has been used to classify the samples into healthy or unhealthy. Block diagram of proposed methodology has been shown in Figure 3.1.

3.2 Preprocessing

First step of any vision system is the image acquisition stage. An Ophthalmoscope has been used to acquire the Fundus image in RGB. Image preprocessing includes image resizing and conversion of RGB image to Gray image.

The Region of Interest (ROI) in the color fundus image is the bright orange-pink area representing Optic Disc. So, in the first part samples are resized to 512x512.

After resizing, images are then converted to gray level. After this, various methods of processing the image can be used to perform different vision tasks.

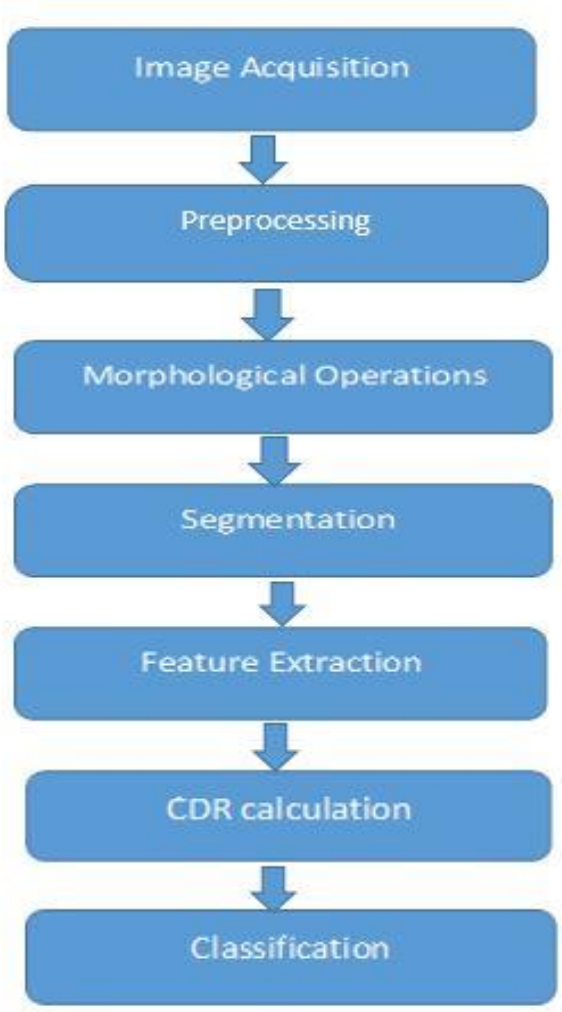

Fig 3.1: Block diagram of the basic methodology used

In Figure 3.2, various stages of preprocessing which includes image resizing and conversion of resized image to gray scale image of a normal and glaucoma fundus images have been depicted.

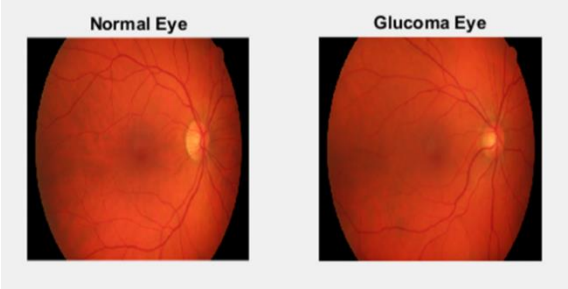

(a)

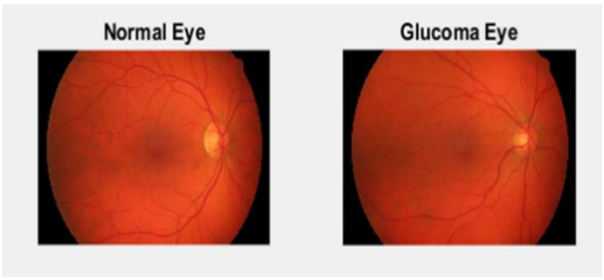

(b)

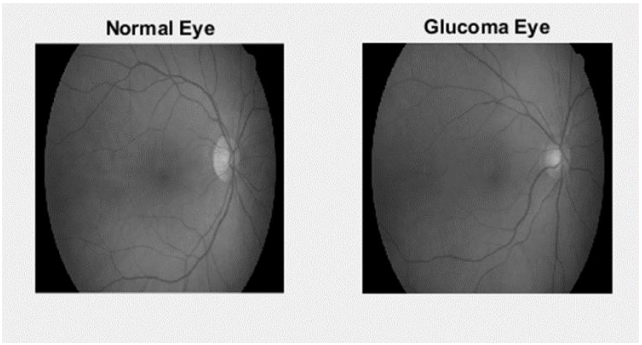

(c)

Fig 3.2 (a) Original images (b) images after resizing (c) Gray scale images

3.3 Extraction

Extraction of OD and OC has been done by converting RGB image to Gray image. Thereafter, morphological operations have been on the image followed by Otsu segmentation. This helps in extraction of optic cup and disc, which is involved in evaluation of CDR.

3.3.1 Extraction of Optic Disc

In Figure 3.3, the methodology for extraction of optic disc has been shown where the obtained image is changed as follows:

3.3.1.1 Image preprocessing

Preprocessing of image is done by converting it from RGB to Gray scale. This pre-processed image undergoes further processing steps.

3.3.1.2 Pre-Gaussian Filter

The Gaussian Filter is a 2D filter which operates on the images by convolution and is used for blurring the images [43]. It also helps in removal of details and noise in the gray image.

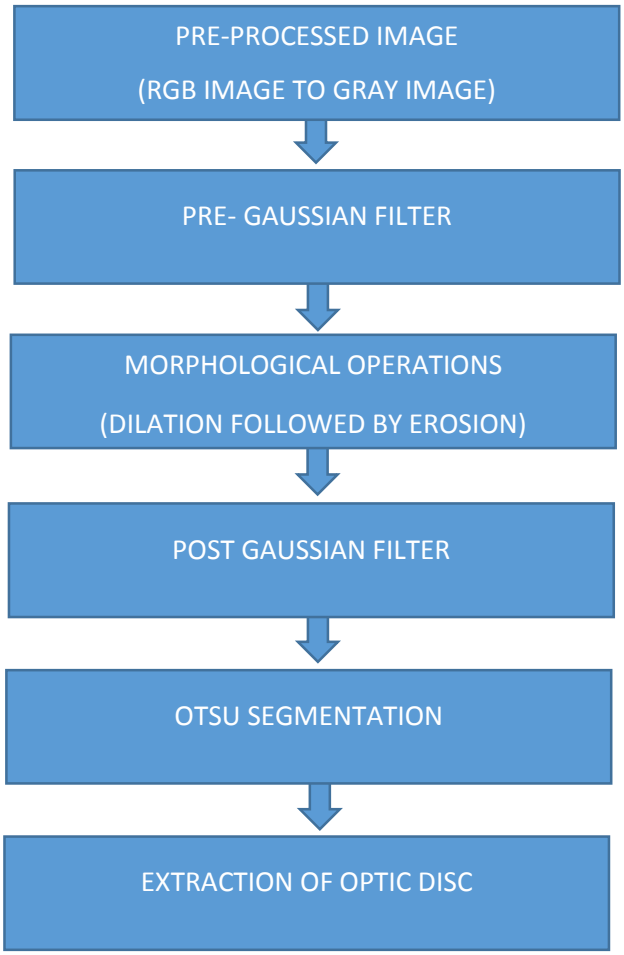

Fig 3.3: Flow diagram for extraction of Optic Disc

3.3.1.3 Morphological Operations

The filtered image has gaps and uneven boundaries which are corrected by applying morphological operations. The "CLOSE" operation is applied on the image through another operation "DISK" which is a structuring element (SE). A structuring element helps in studying, expanding and shaping the image. This operation is called dilation which has been represented in equation 3.1.

The dilation of A by B is defined by:

$$A \oplus B = \cup_{b \in B} A_b \qquad \text{(equation 3.1)}$$

Where A: Binary image

B: structuring element.

Dilation is followed by Erosion where Erosion is an "OPEN" operation. Erosion erodes away the boundaries of forefront part removing structures of certain shapes and leads to shrinking of the image. Erosion has been represented in equation 3.2.

$$A \ominus B = \bigcup_{b \in B} A_{-b} \quad \text{(equation 3.2)}$$

Where A: binary image

B: Structuring element

The CLOSE operation increases the diameter of cup using Dilation, but erosion compensates for this increased diameter because the structural element used is of same dimension. This operation fills in all the gaps and smoothens the contour of the binary image held in the Optic Disc. Sometimes this binary image contains unwanted areas that can be removed using "Area Opening" which gives us a final image that contains the Optic Disc without any unwanted areas.

3.3.1.4 Post-Gaussian Filter

Post Gaussian filter has been used after the morphological operations. Gaussian smoothing filters are commonly used to reduce noise. These are generally isotropic having the same standard deviation along both the dimensions [43].

3.3.1.5 Otsu Segmentation

Segmentation has been done using Otsu's method with multi-level image thresholds. It calculates the optimum threshold on the basis of aggregate bi-modal histogram of the array. Multi thresh uses the RGB fundus image for calculating multi-level image thresholds from three color planes. This represents a 3D numeric array [44].

The threshold values so obtained are represented as positive values. Multi thresh uses Otsu criterion's search-based optimization for finding the thresholds. This optimization gives locally optimum results only. Smaller values of N are used preferably as with an increase in N, the chance of converging to local optimum also increase. N<10 in most of the cases and it cannot be more than 20 [44].

3.3.1.6 Disc Area

After Segmentation, MATLAB inbuilt functions have been used to determine disc area of extracted disc.

3.3.2. Extraction of Optic Cup

It involves the same process with which extraction of optic disc is done after Otsu segmentation. The methodology for extraction of optic cup is shown in figure 3.4

3.3.2.1 Image Preprocessing

Preprocessing of image is done by converting it from RGB to Gray scale. This pre-processed image undergoes further processing steps.

3.3.2.2 Pre-Gaussian Filter

The Gaussian Filter is a 2D filter which operates on the images by convolution and is used for blurring the images [43]. It also helps in removal of details and noise in the gray image.

3.3.2.3 Morphological Operations

The filtered image has gaps and uneven boundaries which are corrected by applying morphological operations. The "CLOSE" operation is applied on the image through another operation "DISK" which is a structuring element (SE). A structuring element helps in studying, expanding and shaping the image. This operation is called dilation which has been represented in equation 3.3.

The dilation of A by B is defined by:

$$A \oplus B = \bigcup_{b \in B} A_b \qquad \text{(equation 3.3)}$$

Where A: Binary image

B: Structuring element

Dilation is followed by Erosion where Erosion is an "OPEN" operation. Erosion erodes away the boundaries of forefront part removing structures of certain shapes and leads to shrinking of the image. Erosion has been represented in equation 3.4.

$$A \ominus B = \bigcup_{b \in B} A_{-b} \qquad \text{(equation 3.4)}$$

Where A: binary image

B: Structuring element

The CLOSE operation increases the diameter of cup using Dilation, but erosion compensates for this increased diameter because the structural element used is of same dimension. This operation fills in all the gaps and smoothens the contour of the binary image held in the Optic Disc. Sometimes this binary image contains unwanted areas that can be removed using "Area Opening" which gives us a final image that contains the Optic Disc without any unwanted areas.

3.3.2.4 Post-Gaussian Filter

Post Gaussian filter has been used after the morphological operations. Gaussian smoothing filters are commonly used to reduce noise. These are generally isotropic having the same standard deviation along both the dimensions [43].

3.3.2.5 Otsu Segmentation

Segmentation has been done using Otsu's method with multi-level image thresholds. It calculates the optimum threshold on the basis of aggregate bi-modal histogram of the array. Multi thresh uses the RGB fundus image for calculating multi-level image thresholds from three color planes. This represents a 3D numeric array. The threshold values so obtained are represented as positive values. Multi thresh uses Otsu criterion's search-based optimization for finding the thresholds. This optimization gives locally optimum results only. Smaller values of N are used preferably as with an increase in N, the chance of converging to local optimum also increase. N<10 in most of the cases and it cannot be more than 20 [44].

3.3.2.6 Cup Area

After Segmentation, MATLAB inbuilt functions has been used to determine disc area of extracted disc.

3.4 Cup to Disc Ratio Calculation

Cup to Disc ratio is calculated as follows

CDR = CUP AREA/DISK AREA

If CDR > 0.5 then eye is unhealthy and if CDR<0.5 then it is considered to be healthy.

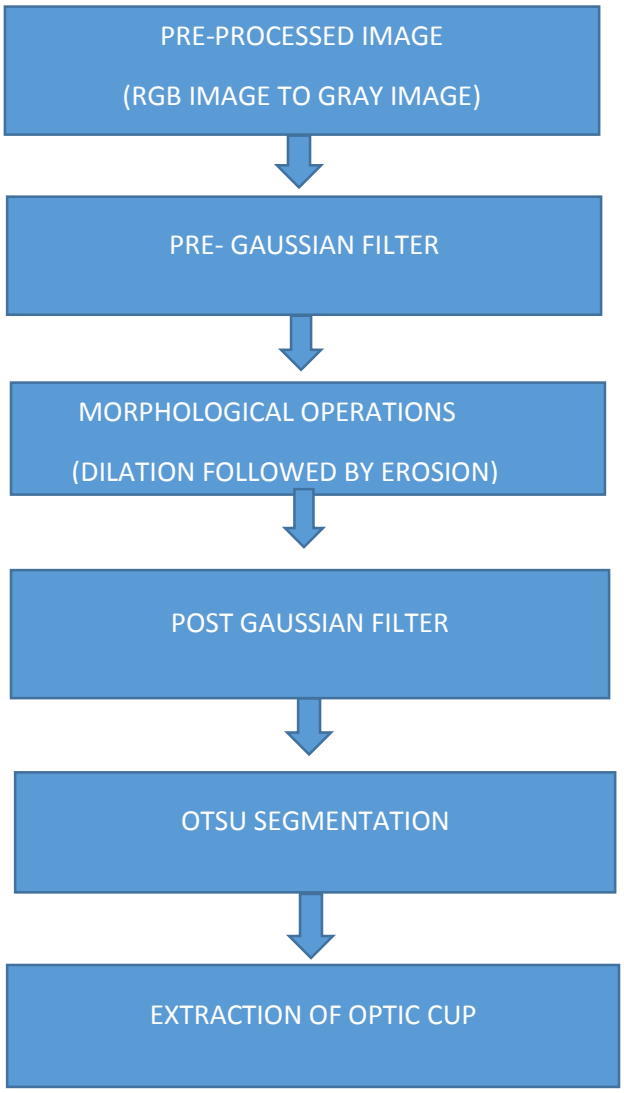

Fig 3.4: Flow diagram for extraction of Optic Cup

3.5 Classification

Support vector machine has been used for classification. In this a hyperplane is constructed which is used to classify the data. SVM has three types of kernels: Linear, Polynomial and Radial basis Gaussian kernel [45].

Out of these three, Radial basis Gaussian kernel has been used in this methodology because this gives the best results. For any two particular feature vectors x and x′, radial basis Gaussian function has been used which is mentioned in equation 3.5 [45].

$$K(x, x') = \exp\left(\left(-||x - x'||\text{^}2\right) / (2\sigma^2)\right) \quad \text{(equation 3.5)}$$

Here, $||x - x'||$ is Euclidean distance between two feature vectors and σ is free parameter, which defines the width or expansion of kernel.

In SVM, if 'n' data points have been trained then they are represented by 'n' vector and 'n' scalar points. In this, the scalar point is either 1 or -1 which in turn corresponds to respective vector point. Support vector machine follows two approaches for classification. One versus One and One versus All. In the proposed methodology one versus all approach has been used.

CHAPTER 4

RESULTS

The database consisting of 120 images, with 18 Healthy and 102 Glaucomatous fundus images have been collected from a local Ophthalmologist and operated upon by the algorithm used.

4.1 Preprocessing Results

As described earlier, Image preprocessing converts the colored retinal image to gray image which is depicted in Fig 4.1.

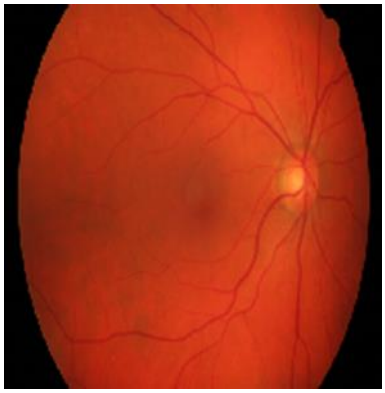

(a)

(b)

Fig. 4.1. (a) RGB image (b) Gray scale image

The Gray images obtained from RGB planes provide the region of interest more conveniently.

4.2 Extraction Results of Optic Disc and Optic Cup

This part discusses the results of proposed methodology for the extraction of Optic Disc and Optic Cup. In this methodology, Gray scale image which have been obtained from image pre-processing is filtered using pre Gaussian filter. After that morphological functions that is dilation followed by erosion have been applied on the image to provide efficient results. Before segmentation and extraction, one more filter is applied that is post Gaussian filter to remove noises.

4.2.1: Pre Gaussian Filter: This is applied after image pre-processing so as to remove any kind of noise in the image. Figure 4.2. depicts the image after the application of Gaussian filter.

Fig 4.2: Result after Pre Gaussian filter

4.2.2: Morphological Operations: In this image undergoes dilation followed by erosion in order to fill gaps and remove blood vessels as we have discussed earlier. Dilated and eroded image has been shown in Figure 4.3 and Figure 4.4 respectively.

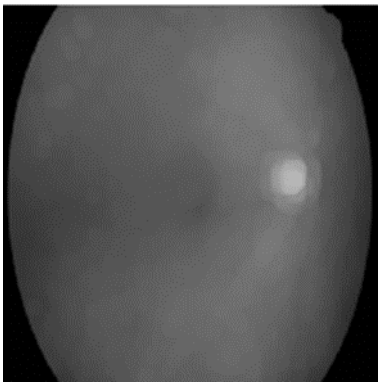

Fig 4.3: Dilated image

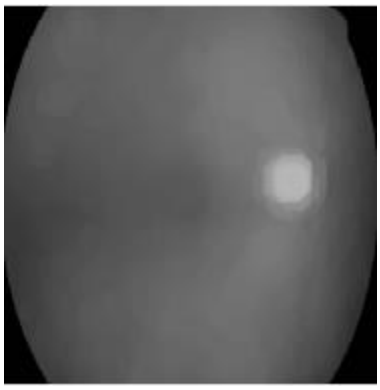

Fig 4.4: Eroded image

4.2.3: Post Gaussian Filter: After applying morphological operations, post Gaussian filter has been applied to ensure that there is no noise in the image and to increase the efficiency. Figure 4.5 depicts the Post Gaussian Filtered image.

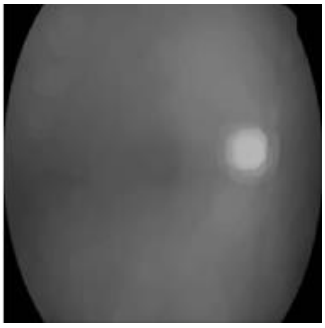

Fig 4.5: Result after Post Gaussian filter

4.2.4: Segmentation: Optic cup and Optic disc has been segmented using Otsu's method for multilevel image thresholds. Segmentation of the filtered image has been shown in Figure 4.6.

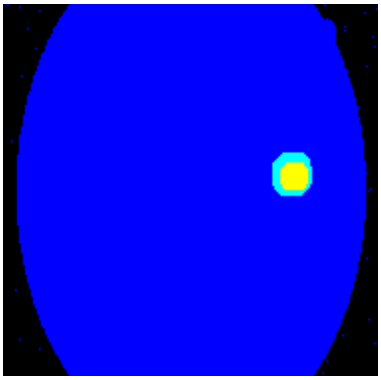

Fig 4.6: Segmented image

4.2.5: Extraction of Optic Disc and Optic Cup: After segmentation the next step is to obtain optic disc and cup. Extraction of Optic Disc and Optic Cup has been shown in Figure 4.7 and Figure 4.8 respectively.

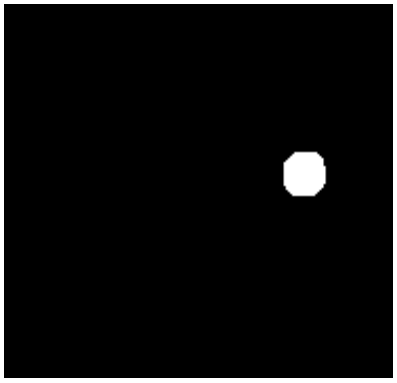

Fig 4.7: Optic Disc

Fig 4.8: Optic Cup

Figure 4.9 and 4.10 shows the various processing stages of some glaucomatous and healthy fundus images out of 120 samples. First column represents processed images. Second column represents gray scale images. Third column represents dilated images. Fourth column represents Post Gaussian filtered image of eroded fundus. Fifth column represents optic cup and Sixth column represents optic disc.

1. 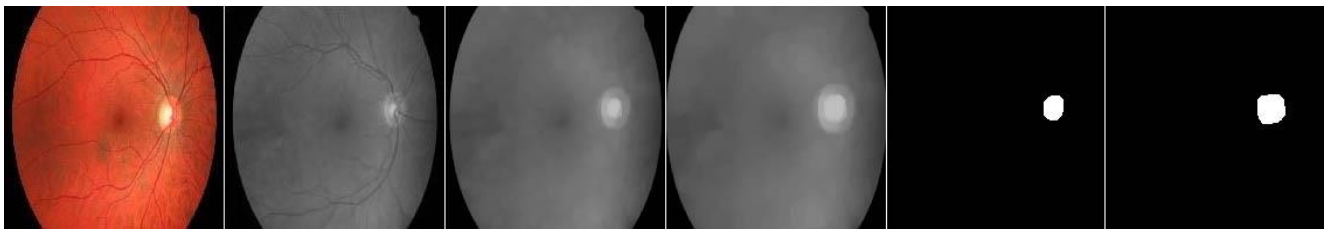

2. 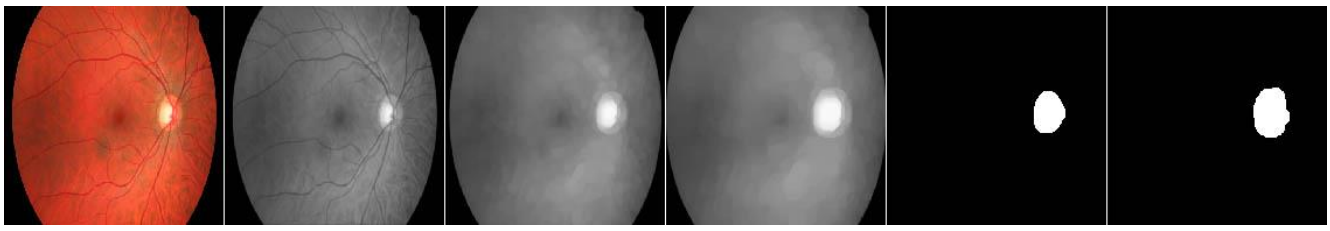

3. 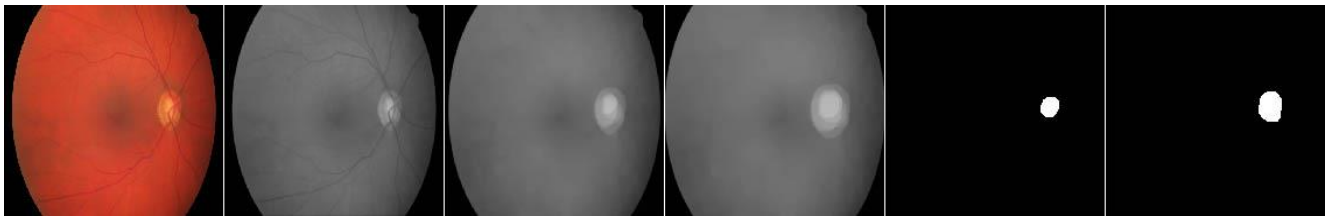

4. 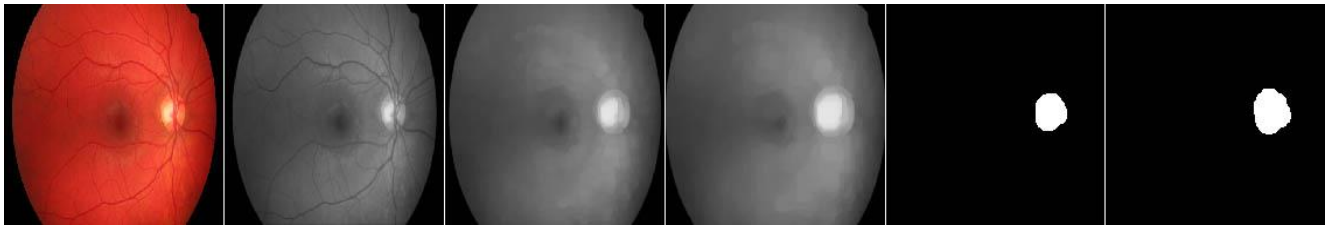

5. 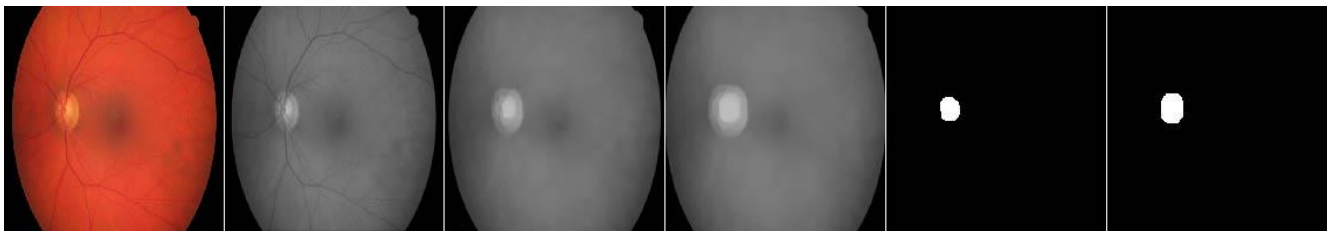

6. 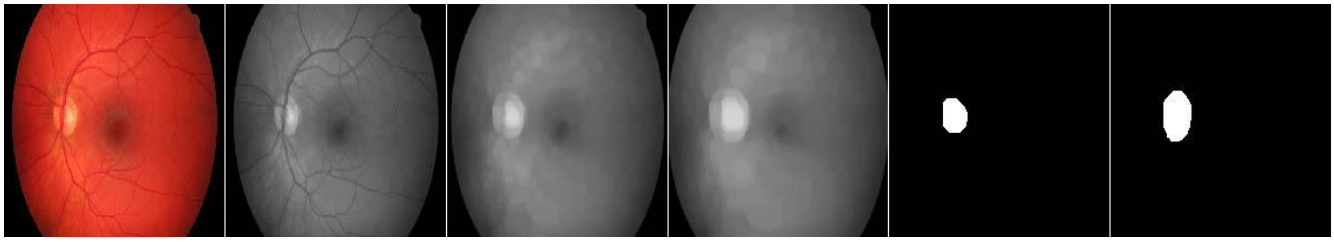

7. 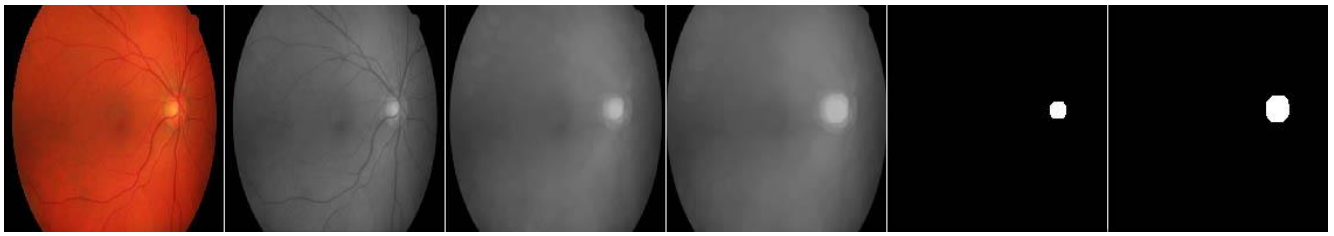

8. 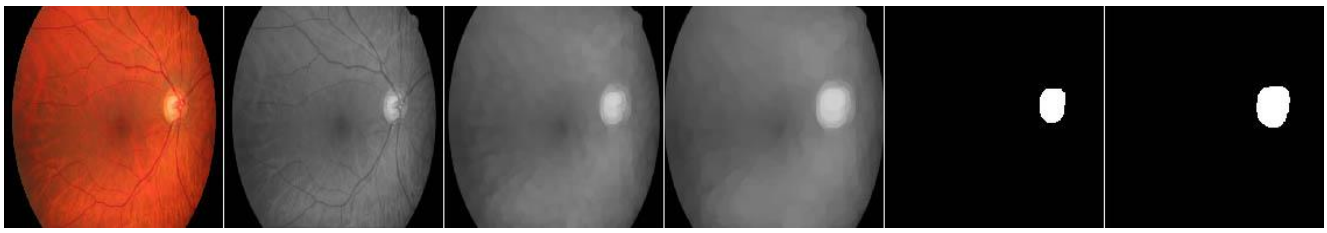

9. 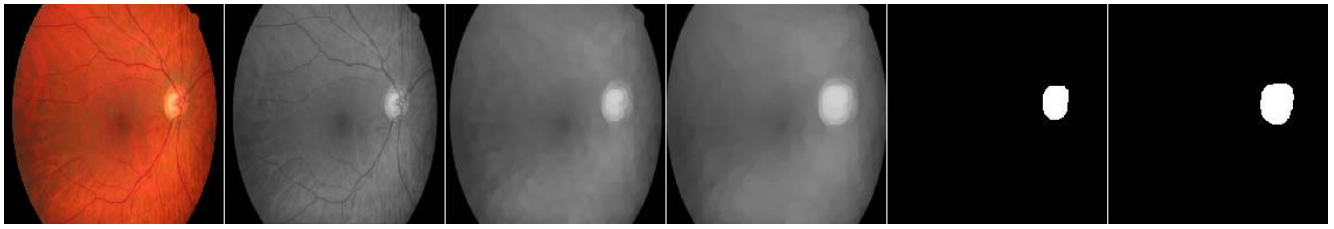

10. 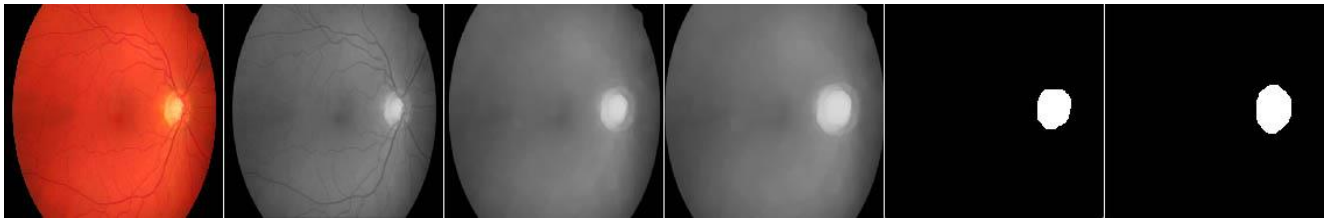

Fig 4.9 Glaucomatous Samples

1. 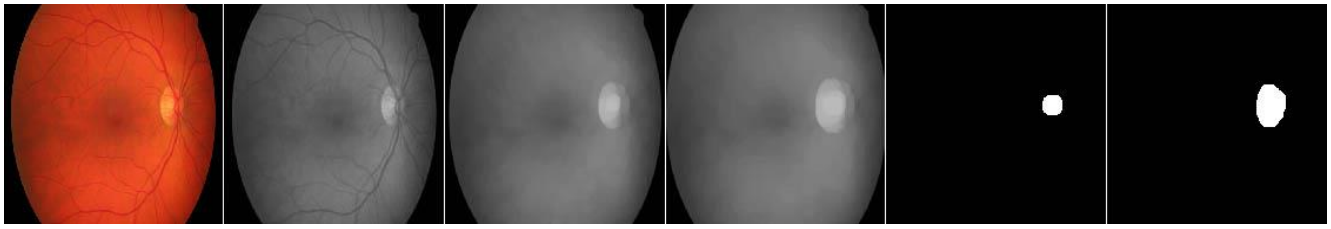

2. 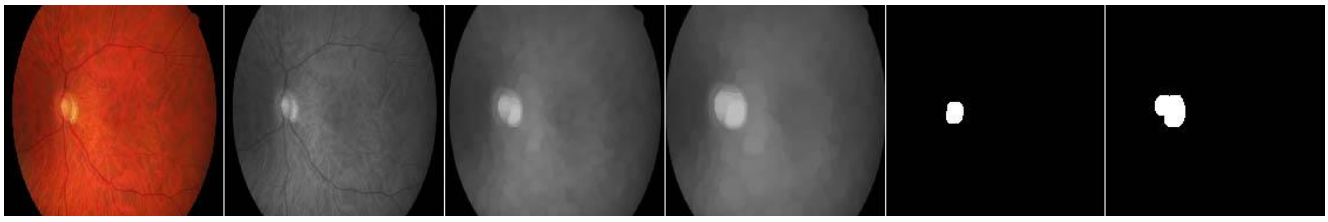

3. 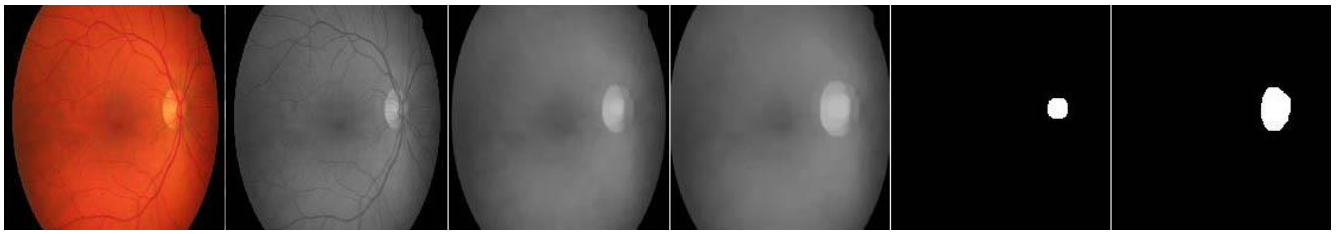

4. 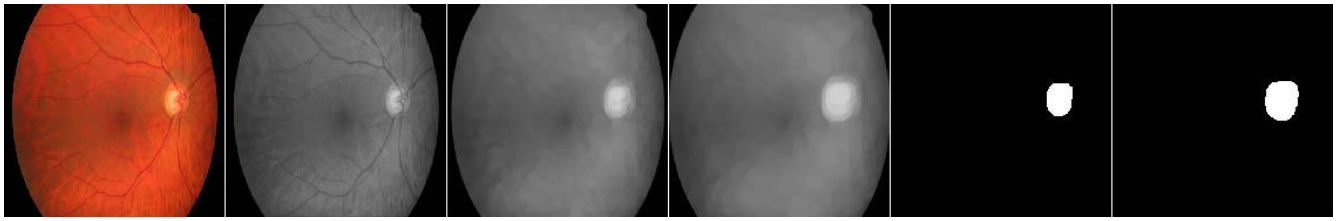

5. 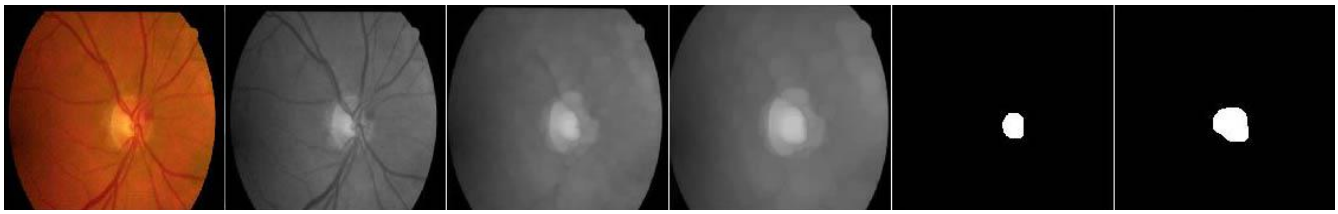

6. 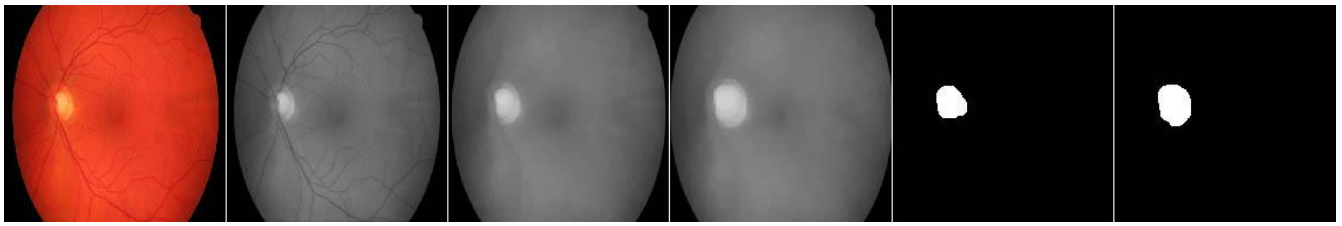

7. 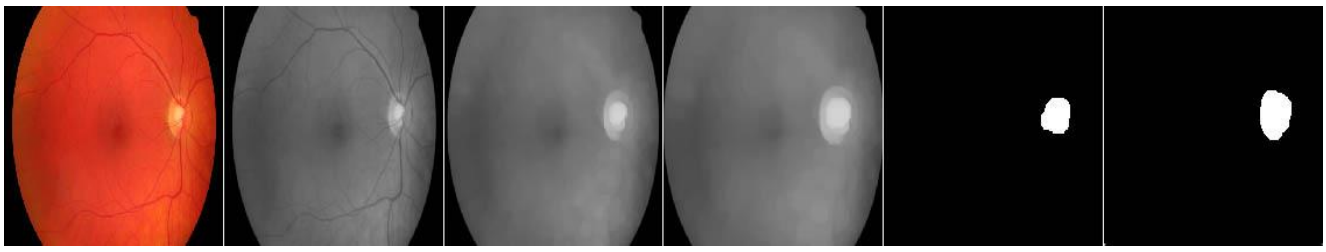

8.

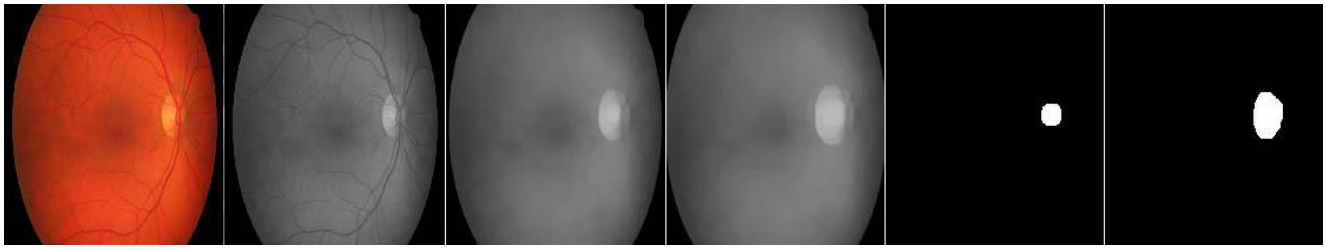

9.

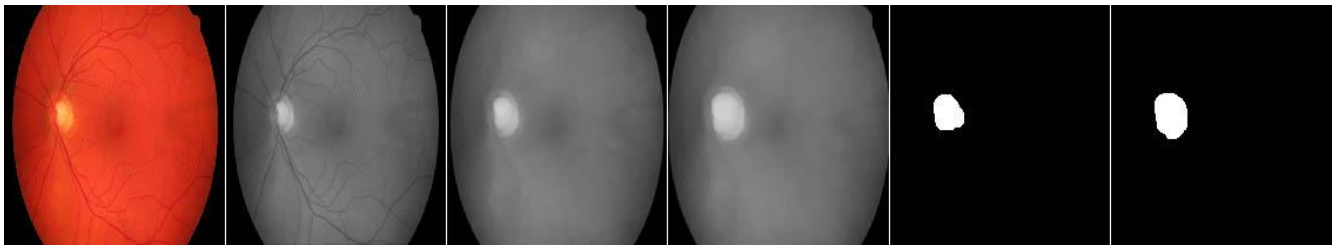

10.

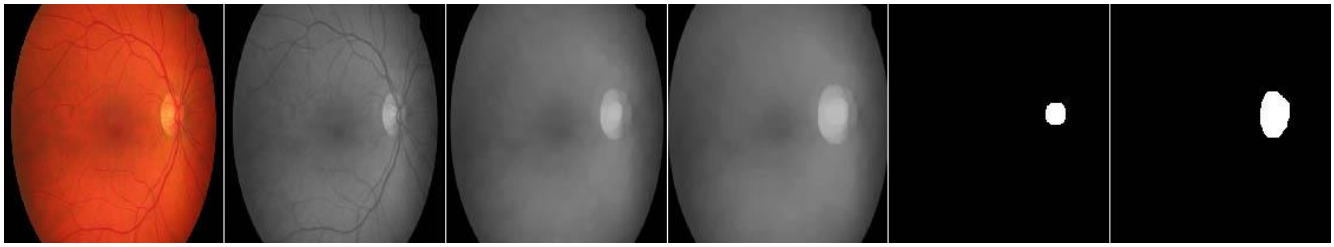

Fig 4.10 Healthy Samples

4.3 Comparison of measured CDR of normal fundus images with true fundus images

For analyzing CDR, SVM using radial basis Gaussian function has been applied and the database has been divided into two classes. Table 4.1 depicts the comparison of measured CDR of normal fundus images with true fundus images.

Table 4.1 Comparison of measured CDR of Normal fundus with true fundus

Sample No	CDR Ratio	Measured	TRUE
1	0.43327	Normal	Normal
2	0.479219	Normal	Normal
3	0.49116	Normal	Normal

4	0.456952	Normal	Normal
5	0.420609	Normal	Normal
6	0.444023	Normal	Normal
7	0.420099	Normal	Normal
8	0.362848	Normal	Normal
9	0.348462	Normal	Normal
10	0.469193	Normal	Normal
11	0.436007	Normal	Normal
12	0.471234	Normal	Normal
13	0.348462	Normal	Normal
14	0.466186	Normal	Normal
15	0.37617	Normal	Normal
16	0.466361	Normal	Normal
17	0.449769	Normal	Normal
18	0.477172	Normal	Normal

4.4 Comparison of measured CDR of glaucomatous fundus images with true images

As discussed earlier, classification of retinal fundus images using SVM has been done. Table 4.2 depicts the comparison of measured CDR of glaucomatous fundus images with true fundus images.

Table 4.2 Comparison of measured CDR of Glaucomatous fundus with true fundus

Sample No.	CDR ratio	Measured	TRUE
1	0.801446	Glaucomatous	Glaucomatous
2	0.673613	Glaucomatous	Glaucomatous
3	0.589567	Glaucomatous	Glaucomatous
4	0.717777	Glaucomatous	Glaucomatous
5	0.696185	Glaucomatous	Glaucomatous
6	0.70871	Glaucomatous	Glaucomatous
7	0.571363	Glaucomatous	Glaucomatous
8	0.57812	Glaucomatous	Glaucomatous
9	0.743165	Glaucomatous	Glaucomatous
10	0.638498	Glaucomatous	Glaucomatous
11	0.645997	Glaucomatous	Glaucomatous
12	0.661155	Glaucomatous	Glaucomatous
13	0.543476	Glaucomatous	Glaucomatous

14	0.729208	Glaucomatous	Glaucomatous
15	0.647935	Glaucomatous	Glaucomatous
16	0.75205	Glaucomatous	Glaucomatous
17	0.813664	Glaucomatous	Glaucomatous
18	0.861032	Glaucomatous	Glaucomatous
19	0.567045	Glaucomatous	Glaucomatous
20	0.69893	Glaucomatous	Glaucomatous
21	0.760805	Glaucomatous	Glaucomatous
22	0.673031	Glaucomatous	Glaucomatous
23	0.85738	Glaucomatous	Glaucomatous
24	0.753999	Glaucomatous	Glaucomatous
25	0.694866	Glaucomatous	Glaucomatous
26	0.557897	Glaucomatous	Glaucomatous
27	0.769989	Glaucomatous	Glaucomatous
28	0.803559	Glaucomatous	Glaucomatous
29	0.896019	Glaucomatous	Glaucomatous
30	0.643343	Glaucomatous	Glaucomatous

31	0.627265	Glaucomatous	Glaucomatous
32	0.7463	Glaucomatous	Glaucomatous
33	0.642815	Glaucomatous	Glaucomatous
34	0.739236	Glaucomatous	Glaucomatous
35	0.837138	Glaucomatous	Glaucomatous
36	0.71172	Glaucomatous	Glaucomatous
37	0.63851	Glaucomatous	Glaucomatous
38	0.57127	Glaucomatous	Glaucomatous
39	0.771966	Glaucomatous	Glaucomatous
40	0.781401	Glaucomatous	Glaucomatous
41	0.535905	Glaucomatous	Glaucomatous
42	0.568897	Glaucomatous	Glaucomatous
43	0.746273	Glaucomatous	Glaucomatous
44	0.70958	Glaucomatous	Glaucomatous
45	0.760106	Glaucomatous	Glaucomatous
46	0.722422	Glaucomatous	Glaucomatous
47	0.590066	Glaucomatous	Glaucomatous

48	0.59726	Glaucomatous	Glaucomatous
49	0.709771	Glaucomatous	Glaucomatous
50	0.772532	Glaucomatous	Glaucomatous
51	0.768458	Glaucomatous	Glaucomatous
52	0.832501	Glaucomatous	Glaucomatous
53	0.551991	Glaucomatous	Glaucomatous
54	0.738801	Glaucomatous	Glaucomatous
55	0.523184	Glaucomatous	Normal
56	0.742402	Glaucomatous	Glaucomatous
57	0.631395	Glaucomatous	Glaucomatous
58	0.658324	Glaucomatous	Glaucomatous
59	0.533164	Glaucomatous	Glaucomatous
60	0.656786	Glaucomatous	Glaucomatous
61	0.816311	Glaucomatous	Glaucomatous
62	0.704411	Glaucomatous	Glaucomatous
63	0.770075	Glaucomatous	Glaucomatous
64	0.720758	Glaucomatous	Glaucomatous

65	0.566289	Glaucomatous	Glaucomatous
66	0.728791	Glaucomatous	Glaucomatous
67	0.648878	Glaucomatous	Glaucomatous
68	0.748147	Glaucomatous	Glaucomatous
69	0.834712	Glaucomatous	Glaucomatous
70	0.808152	Glaucomatous	Glaucomatous
71	0.766945	Glaucomatous	Glaucomatous
72	0.854502	Glaucomatous	Glaucomatous
73	0.717156	Glaucomatous	Glaucomatous
74	0.843493	Glaucomatous	Glaucomatous
75	0.533164	Glaucomatous	Glaucomatous
76	0.724537	Glaucomatous	Glaucomatous
77	0.88375	Glaucomatous	Glaucomatous
78	0.633046	Glaucomatous	Glaucomatous
79	0.743097	Glaucomatous	Glaucomatous
80	0.914347	Glaucomatous	Glaucomatous
81	0.609762	Glaucomatous	Glaucomatous

82	0.59389	Glaucomatous	Glaucomatous
83	0.851213	Glaucomatous	Glaucomatous
84	0.742793	Glaucomatous	Glaucomatous
85	0.581596	Glaucomatous	Glaucomatous
86	0.848369	Glaucomatous	Glaucomatous
87	0.844857	Glaucomatous	Glaucomatous
88	0.61882	Glaucomatous	Glaucomatous
89	0.61505	Glaucomatous	Glaucomatous
90	0.620806	Glaucomatous	Glaucomatous
91	0.825248	Glaucomatous	Glaucomatous
92	0.534825	Glaucomatous	Glaucomatous
93	0.564181	Glaucomatous	Glaucomatous
94	0.63904	Glaucomatous	Glaucomatous
95	0.860226	Glaucomatous	Glaucomatous
96	0.789268	Glaucomatous	Glaucomatous
97	0.77997	Glaucomatous	Glaucomatous
98	0.662131	Glaucomatous	Glaucomatous

99	0.757077	Glaucomatous	Glaucomatous
100	0.760791	Glaucomatous	Glaucomatous
101	0.830687	Glaucomatous	Glaucomatous
102	0.641323	Glaucomatous	Glaucomatous

4.5 Parameters Evaluation

The conclusion of the proposed methodology to classify the samples is based on image quality and experience of the physician. Thus a confusion matrix is applied to analyze the performance of algorithm used [46]. This matrix consists of predicted class and actual class which are illustrated in fig. 4.11.

Here,

True positive (TP) – the number of samples which are actually affected

True Negative (TN) – the number of samples which are actually normal samples

False Negative (FN) – the number of samples which are incorrectly labelled as normal

False Positive (FP) – the number of samples which are incorrectly labelled as affected

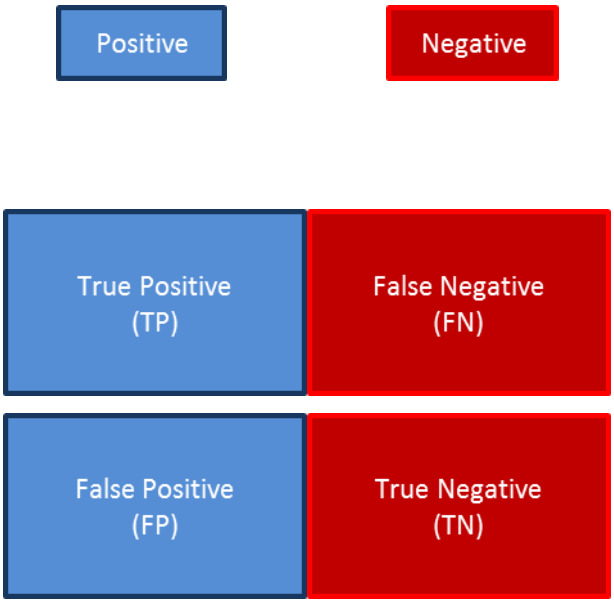

Fig.4.11 Plotted Confusion Matrix

The confusion matrix with proposed algorithm specimen has been shown in Figure 4.12. Formulation of predictive parameters to evaluate performance of algorithm has been done by using these specimen.

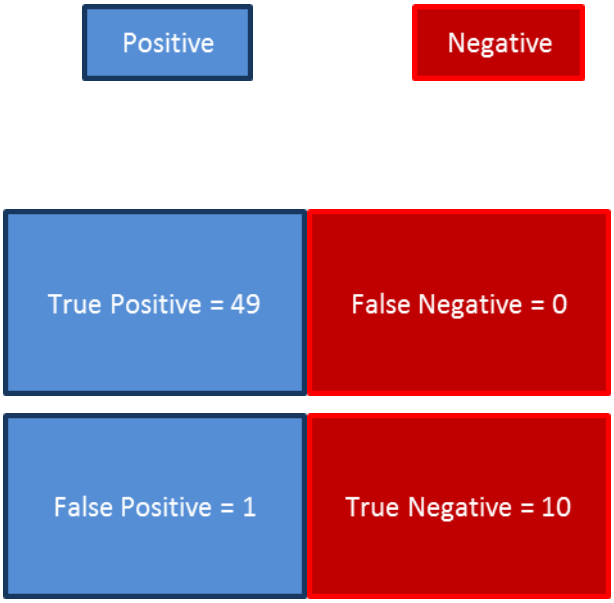

Fig. 4.12 Confusion Matrix with Algorithm specimen

Various Parameters used for evaluation and visualization of algorithm's performance are as follows:

4.5.1 Specificity

It calculates the true negative section which is correctly labelled. Thus it is also called True Negative Rate. It is measured as ratio of true negative to the sum of true negative and false positive.

$$Specificity = TN / (TN + FP)$$

4.5.2 Sensitivity

It calculates true positive section which is correctly labelled. Thus it is also called True Positive Rate. It is measured as the ratio of true positive to the sum of true positive and false negative.

$$Sensitivity = TP / (TP + FN)$$

4.5.3 Accuracy

Accuracy signifies the relation between calculated and true values. It is represented as

$$Accuracy = (TP + TN) / (TP + TN + FP + FN)$$

4.5.4 Precision

It is also known as Positive Predictive Value (PPV). It is the measure of efficiency of the algorithm to determine the samples correctly. It is calculated as

$$PPV = TP / (TP + FP)$$

4.5.5 Negative Predictive Value

In the results, negative proportion is depicted by NPV.

$$NPV = TN / (TN + FN)$$

4.5.6 False Positive Rate

It represents the chances of false rejection of any relation between evaluated groups. It can be measured as

$$FPR = FP / (FP + TN)$$

4.5.7 False Negative Rate

It falsely shows negative results i.e. the absence of disease while it is present actually. It can be calculated as

FNR= FN/ (FP+TP)

4.5.8 False Discovery Rate

FDR determines the percentage of predictions which are false out of various predictions. It is denoted as follows

FDR= FP/ (FP+TP)

4.5.9 F1 Score

It denotes how accurately the algorithm works.

F1 Score= 2TP/ (2TP+FP+FN)

Table 4.3 and Table 4.4 depicts Predictive Parameter Values and Test Outcomes respectively.

Table 4.3: Predictive Parameter Values

TP	FP	TN	FN
49	1	10	0

Table 4.4: Test Outcomes

S. No.	**Parameter**	**Value**
1	Percentage Accuracy	98.33
2	Percentage Sensitivity	100
3	Percentage Specificity	90.90
4	PPV	0.98
5	NPV	1
6	Percentage FPR	9

7	Percentage FDR	2
8	Percentage FNR	0
9	F1 score	0.98

Figure 4.13, depicts the test outcomes where accuracy is 98.33%, sensitivity is 100% and specificity is 90.90%.

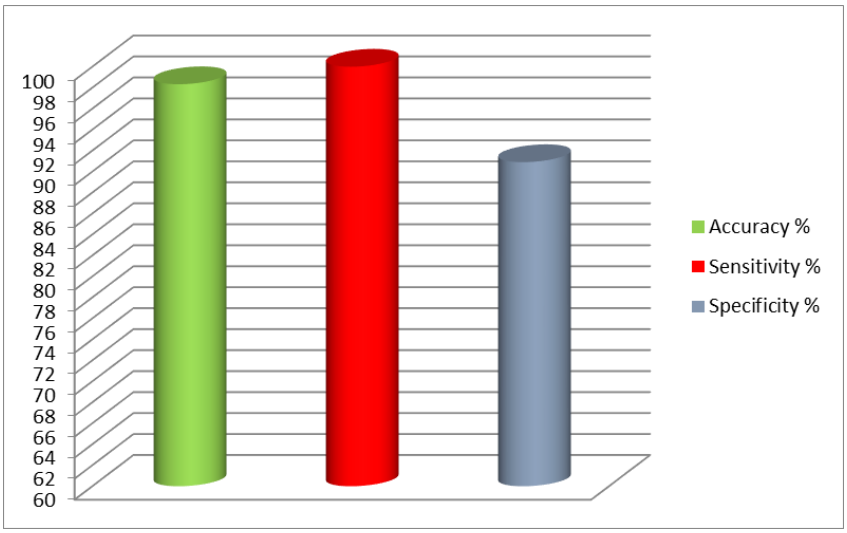

Fig 4.13 Accuracy, sensitivity & specificity percentage of samples

Percentage Graph representation of false positive rate, false discovery rate and false negative rate has been shown in Fig 4.14.

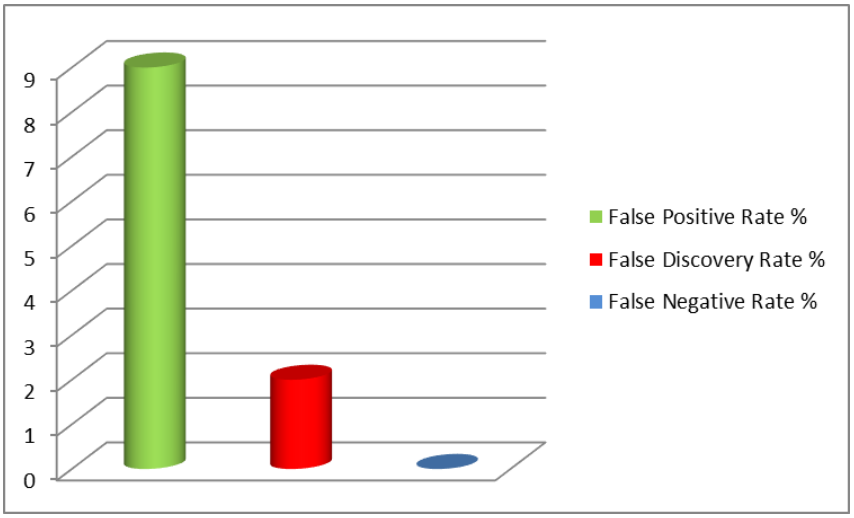

Fig 4.14 FPR, FDR & FNR percentage of samples

Figure 4.15 represents the graph of precision, negative prediction value and F1 score of the database taken.

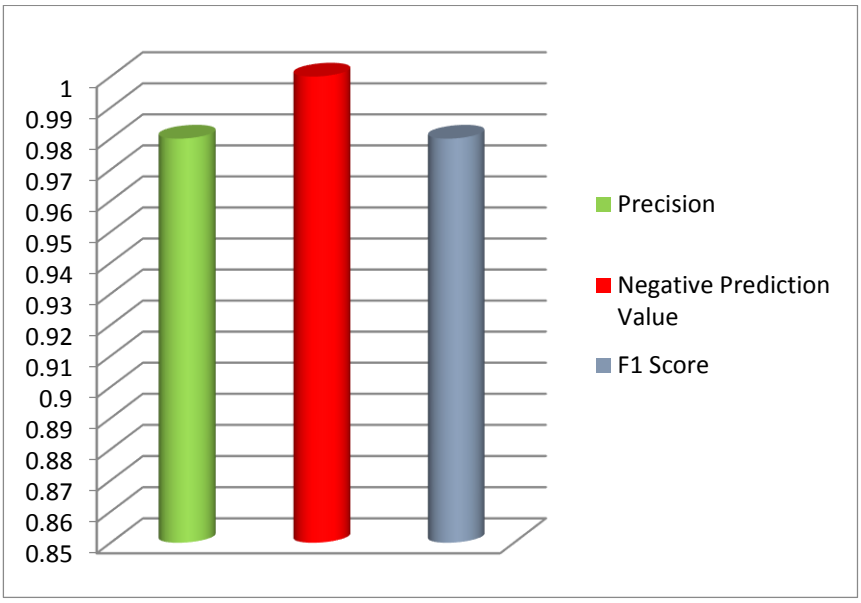

Fig 4.15 Precision, NPV & F1 score of samples

.

CHAPTER 5

CONCLUSION

5.1 Conclusion

Glaucoma is a grave disease of eye which irreversibly damages the optic nerve leading to severe consequences. So, it is important to detect it at early stage for which various methodologies have been developed, CDR being one of them. In this research work, 120 samples of retinal fundus images have been taken. These image samples have been worked upon by MATLAB R2015a. Out of 120, 60 samples have been tested while rest are trained. The CDRs of tested samples has been checked against trained samples and it has been found that 59 out 60 samples are correctly classified. The presented algorithm showed 98.33% of accuracy and 100% of sensitivity.

If the CDR is less than 0.5, retinal fundus is said to be normal. But if it exceeds 0.5 then it is said to be at risk. Average value of CDR for normal subjects is 0.4 approximately while for affected ones it is around 0.7.

5.2 Future Scope

The future scope for the dissertation can be the investigation of more contrasting features for the confirmation of suspicious samples. This can be done as follows:

- Checking the area of ISNT quadrants as per ISNT rule
- Analysis of Neuro- Retinal Rim (NRR).
- By measuring intra-ocular pressure known as Tonometry.
- Inspection of drainage angle of the eye known as Gonioscopy.
- Visual field examination known as Perimetry.

REFERENCES

[1] M. Singh, Introduction to Biomedical Instrumentation, PHI Learning Pvt. Ltd., PP: 5-6, 2010.

[2] Rhee, Douglas J. Porter, Robert S.; Kaplan, Justin L., eds."Glaucoma". The Merck Manual Home Health Handbook. PP: 4-5 December 12, 2013.

[3] Glaucoma: Causes, Risk Factors, Symptoms, Diagnosis and Treatment, Available at:http://www.southernophthalmology.com.au/glaucoma.html#glaucoma.

[4] H. Li, O. Chutatape, "A Model-Based Approach for Automated Feature Extraction in Fundus Images", Computer Vision Proceedings. Ninth IEEE International Conference, pp. 394 - 399 Vol.1, 2003.

[5] J. Liu1, D. W. K. Wong1, J.H. Lim1, X. Jia1, F. Yin1, H. Li1, W. Xiong1, T. Y. Wong2, "Optic Cup and Disk Extraction from Retinal Fundus Images for Determination Of Cup-To-Disc Ratio", IEEE Conference on Industrial Electronics and Applications, 2008.

[6] Damage to Optic Nerve due to Increased Eye pressure, Available at: http://en.dunyagoz.com/treatments/glaucoma-high-eye-pressure.html?print=1

[7] Primary Open Angle Glaucoma, Available at https://www.glaucomafoundation.org/Primary_OpenAngle_Glaucoma.htm

[8] Aqueous Fluid Pathway, Available at: http://www.naturaleyecare.com/ocularsupport/optic-nerve-support/intraocular-pressure.asp.

[9] Primary open angle glaucoma diagram, Available at: https://www.google.co.in/search?q=primary+open+angle+glaucoma+diagram.

[10] Joshua D. Stein, MD, MS, and Pratap Challa, MD. Available at: http://www.aao.org/eyenet/article/diagnosis-treatment-of-normal-tension-glaucoma?february-2007

[11] Angle Closure Glaucoma Available at: http://www.glaucoma.org/glaucoma/angle-closure-glaucoma.php.

[12] Acute Angle Glaucoma Available at: http://patient.info/in/health/acute-angle-closure-glaucoma.

[13]Pigmentary Glaucoma Available at https://www.glaucomafoundation.org/pigmentary_glaucoma.htm

[14] Glaucoma and your eyes, Available at: http://www.webmd.com/eye-health/glaucomaeyes

[15] Exfoliation Syndrome Available at: https://www.glaucomafoundation.org/exfoliation_syndrome.htm

[16] Normal Fundus, Available at: http://homedesignblogs.net/tag/fundus-definition-offundus-by-medical-dictionary

[17] Healthy and Unhealthy Optic Disk, Available at: http://galleryhip.com/open angle glaucoma- cup-to-disc-ratio.html.

[18] ISNT Quadrants, Available at: http://www.ijo.in/article.asp?issn.

[19] J. Lowell, A. Hunter, D. Steel, A. Basu, R. Ryder, E. Fletcher, and L. Kennedy, "Optic nerve head segmentation", IEEE Transactions on Medical Imaging , Vol 23, pp. 256 –264, 2004.

[20] K. Noronha, J. Nayak, S. N. Bhatt, "Enhancement of retinal fundus image to highlight the features for detection of abnormal eyes", 10th Conference in IEEE, pp. 1- 4, 2006.

[21] Peng Feng, Ying jun Pan, Wei Jin, Baio Wei and Deling Mi, "Enhancing Retinal Image by the Countourlet Transform", Pattern Recognition Letters (Elsevier), Vol.28, 2007.

[22] S. Sekhar, W. A. Nuaimy and A. K. Nandi "Automated Localisation Of Retinal Optic Disk Using Hough Transform", Biomedical Imaging: From Nano to Macro, 2008, 978-1- 4244-2002-5, pp. 1577-1580, 2008.

[23] G. B. Kande, P. V. Subbaiah, T. S. Savithri, "Feature Extraction in Digital Fundus Images", Journal of Medical and Biological Engineering, Vol 29, Issue 3, pp. 122-130, 2009.

[24] A.W. Reza, C. Eswaran, S. Hati " Automatic Tracing Of Optic Disc And Exudates From Color Fundus Images Using Fixed And Variable Thresholds", Journal of Medical Systems, Vol. 33, Issue. 1, pp. 73-80, 2009.

[25] J. Nayak, R. Acharya, U. P. S. Bhat, N. Shetty, T. C. Lim, "Automated Diagnosis of Glaucoma Using Digital Fundus Images", Volume 33 Issue 5, pp. 337 – 346, 2009.

[26] S. Ravishankar, A. Jain, and A. Mittal, "Automated feature extraction of early detection of diabetic retinopathy in fundus images", International Conference in IEEE, pp 210- 220, 2009.

[27] R. Bock, J. Meier, L. G. Nyúl , J. Hornegger , G. Michelson, "Glaucoma risk index: Automated glaucoma detection from color fundus images", Medical Image Analysis, Vol 14, pp. 471–481, 2010.

[28] A. Aquino, M. E. G. Arias, and D. Marín, "Detecting The Optic Disc Boundary In Digital Fundus Images Using Morphological, Edge Detection, And Feature Extraction Techniques", IEEE Transactions On Medical Imaging, Vol 29 Issue 11, pp. 1860-1869, 2010.

[29] D. W. K. Kong, J. Liu, N. M. Tan, F. Yin, B. H. Lee, and T. Y. Wong, "Learning based approach for the automatic detection of the optic disc in retinal fundus photograph", 32nd Annual International Conference of the IEEE, pp. 5355 – 5358, 2010.

[30] E. Mahfouz, and A. S. Fahmy," Fast Localization of the optic disc using projection of image features", IEEE Transactions on Image Proceedings, Vol 19, pp. 3285 – 3289, 2010.

[31] P. C. Siddalingaswamy, and K. G. Prabhu, "Automated grading of diabetic maculopathy severity levels", Proceedings of International Conference on Systems in Medicine and Biology, pp. 331 – 334, 2010.

[32] M. Mishra, M. K. Nath and S. Dandapat, "Glaucoma Detection From Color Fundus Images", International Journal of Computer & Communication Technology, Vol 2 Issue 6, 2011.

[33] A.W. Reza, C. Eswaran, S. Hati " Automatic Tracing Of Optic Disc And Exudates From Color Fundus Images Using Fixed And Variable Thresholds", Journal of Medical Systems, Vol. 33, Issue 1, pp. 73-80, 2009.

[34] F. Yin, J. Liu, S. H. Ong, Y. Sun, Damon W. K. Wong, N. M. Tan, C. Cheung, M. Baskaran, T. Aung, T. Y. Wong, "Model based optic nerve head segmentation on retinal fundus images", 33rd Annual International Conference of the IEEE, pp. 2626 – 2629, 2011.

[35] J. Cheng, J. Liu, D. W. K. Wong, F. Yin, C. Cheung, M. Baskaran, T. Aung, and T. Y. Wong, "Automatic optic disc segmentation with peripapillary atrophy elimination", 33rd International Conference of the IEEE, pp. 6224 – 6227, 2011.

[36] Dehgani, H. A. Moghaddam, M. S. Moin, "Optic disc localization in retinal images using histogram matching", Journal on Image and Video Processing, pp. 2012 – 2019, 2012.

[37] M. Esameili, H. Rabbani, A. M. Dehnavi, and A. Dehghani , " Automatic detection of exudates and optic disk in retinal images using curvelet transform", IET Image Process, Vol 6, pp. 1005 – 1013, 2012.

[38] S.Kavitha , K.Duraiswamy, "An Efficient Decision Support System Detection Of Glaucoma In Fundus Images Using Anfis", International Journal Of Advances In Engineering & Technology, Vol. 2, Issue 1, pp. 227-240, 2012.

[39] H. Yu, E. S. Barriga, C. Agurto, S. Echegaray, M. S. Pattichis, W. Bauman, and P. Soliz, “Fast localization and segmentation of optic disc in retinal images using directional matched filtering and level sets”, IEEE Transactions on Information Technology in Biomedicine, Vol 16, pp 644 – 657, 2012.

[40] M.R.S.P. Kumara and R. G. N. Meegama. "Active contour-based segmentation and removal of optic disk from retinal images", In Advances in ICT for Emerging Regions (ICTer), 2013 International Conference, pp. 15-20, 2013.

[41] F. Khan, S. A. Khan, U. U. Yasin, I. ul Haq, U. Qamar, “Detection of Glaucoma Using Retinal Fundus Images”, The 2013 Biomedical Engineering International Conference, 2013.

[42] S. Gonzalez, D. Kaba, Y. Li and X. Liu, “Segmentation of blood vessels and optic disc in retinal images”, IEEE Journal of Biomedical and Health Informatics, pp. 1-14, 2014.

[43] Gaussian filter Available at: https://en.wikipedia.org/wiki/Gaussian_filter.

[44] Otsu segmentation Available at: https://en.wikipedia.org/wiki/Otsu%27s_method

[45] Support vector machine Available at: https://en.wikipedia.org/wiki/Support_vector_machine

[46] Powers, David M W, "Evaluation: From Precision, Recall and F-Measure to ROC Informedness, Markedness & Correlation" (PDF). *Journal of Machine Learning Technologies*, Vol **2**, Issue 1, pp. 37–63, 2011.

PLAGIARISM REPORT

ORIGINALITY REPORT

5%	2%	4%	0%
SIMILARITY INDEX	INTERNET SOURCES	PUBLICATIONS	STUDENT PAPERS

PRIMARY SOURCES

1	Ahmed, S.S.S.J.. "Neural network algorithm for the early detection of Parkinson's disease from blood plasma by FTIR micro-spectroscopy", Vibrational Spectroscopy, 20100720 Publication	1%
2	Shulin, Cui, and Zhang Shuqing. "An Image Decomposition Strategy Based on GUP's Memory Hierarchy Architecture", 2013 International Conference on Computational and Information Sciences, 2013. Publication	<1%
3	Khan, Fauzia, Shoaib A. Khan, Ubaid Ullah Yasin, Ihtisham ul Haq, and Usman Qamar. "Detection of glaucoma using retinal fundus	<1%

images", The 6th 2013 Biomedical Engineering International Conference, 2013.
Publication

4	www.ukessays.com Internet Source	<1%
	turk-jem.dergisi.org Internet Source	<1%
6	www.premseyeclinic.com Internet Source	<1%
7	The Glaucomas, 2014. Publication	<1%
8	en.wikipedia.org Internet Source	<1%
9	Jose, Asha Merin, and Arun A. Balakrishnan. "A novel method for glaucoma detection using optic disc and cup segmentation in digital retinal fundus images", 2015 International Conference on Circuits Power and Computing Technologies [ICCPCT-2015], 2015. Publication	<1%
		<1%

10	Anis Karimpour-Fard. "Predicting protein linkages in bacteria: Which method is best depends on task", BMC Bioinformatics, 2008 Publication	
11	Ahmad, Hafsah, Abubakar Yamin, Aqsa Shakeel, Syed Ormer Gillani, and Umer Ansari. "Detection of glaucoma using retinal fundus images", 2014 International Conference on Robotics and Emerging Allied Technologies in Engineering (iCREATE), 2014 Publication	<1%
12	"Pearls of Glaucoma Management", Springer Nature, 2016 Publication	<1%
13	www.ijcaonline.org Internet Source	<1%
14	www.ijisme.org Internet Source	<1%
15	www.tdx.cat Internet Source	<1%